On kannemeyeriiform dicynodonts from the *Shaanbeikannemeyeria* Assemblage Zone of the Ordos Basin, China

LIU Jun[1,2]

(1 *Key Laboratory of Vertebrate Evolution and Human Origins of Chinese Academy of Sciences*, *Institute of Vertebrate Paleontology and Paleoanthropology*, *Chinese Academy of Sciences* Beijing 100044 liujun@ivpp.ac.cn)
(2 *College of Earth and Planetary Sciences*, *University of Chinese Academy of Sciences* Beijing 100049)

Abstract *Shaanbeikannemeyeria* is a common tetrapod from the lower part of the Ermaying Formation of the Ordos Basin, China. There are taxonomical questions surrounding this genus, such as the validity of the genus, and how many species are included within it. Several specimens have been collected since 1978. *Shaanbeikannemeyeria* first appeared from the top of the Heshanggou Formation. These specimens are described to clarify the diagnostic characters, the individual variations and the phylogenetic position of *Shaanbeikannemeyeria*. Only one species, *S. xilougouensis*, is recognized. It is characterized by the following autapomorphies: occiput strongly inclined relative to the palate such that the skull is much shorter basally than dorsally, sword tip-like premaxillary posterodorsal processes, tall and dorsally-convex cutting blade on the medial edge of the dorsal surface of the dentary, reflected lamina with a separated posteroventral process, and 15 dorsal vertebrae. This species shows variations on the cranial morphology, such as the occiput height relative to the width, the snout tip (sharp or obtuse), the shape of the orbital portion of the zygomatic arch, and the shape of caniniform process. Some variations could be ontogenetically related, such as the development of the caniniform process and tusk, the posterior extension of the maxilla on the zygomatic arch, the distance between the frontal and the premaxilla, the intertemporal bar width, and the exposing degree of the parietals. Based on postcranial bones, the second dicynodont genus (possibly *Parakannemeyeria*) is present in the lower Ermaying Formation.

Key words Heshanggou Formation, Ermaying Formation, Middle Triassic, Anisian, Kannemeyeriiformes

Citation Liu J, in press. On kannemeyeriiform dicynodonts from the *Shaanbeikannemeyeria* Assemblage Zone of the Ordos Basin, China. Vertebrata PalAsiatica.

中科院国际合作局对外合作重点项目(132311KYSB20190010)和中国科学院战略性先导科技专项(B类)(XDB26000000)资助。

收稿日期：2022-01-26

1 Introduction

During 1962–1964, Cheng Zhen-Wu from the Institute of Geology, Chinese Academy of Geological Sciences (IGCAGS) collected many Permo-Triassic vertebrate fossils from the Ordos Basin. Based on these fossils, he established several new taxa including *Shaanbeikannemeyeria xilougouensis* from Fugu County, Shaanxi Province (Cheng, 1980). In 1976 and 1977, the Institute of Vertebrate Paleontology and Paleoanthropology, Chinese Academy of Sciences (IVPP) sent a field team to Junger Banner, Nei Mongol and discovered fossil-bearing layers from the Heshanggou Formation and the lower part of the Ermaying Formation, which produced a diverse tetrapod fauna. An incomplete skeleton from Buerdong (locality 76014) was referred to *Shaanbeikannemeyeria* as the holotype of *S. buerdongia* (Li, 1980). Recently, it has been regarded as a junior synonym of *S. xilougouensis* (Li and Liu, 2015). In the area of Gucheng-Buerdong, *Shaanbeikannemeyeria* is the only known dicynodont from the lower Ermaying Formation. However, around 100 km south to this area, *Parakannemeyeria xingxianensis* was reported from the lower Ermaying Formation (Cheng, 1980).

Shaanbeikannemeyeria is a common tetrapod within the fossil-bearing strata and tetrapod assemblage zones have been named based on this genus (Li and Cheng, 1995; Liu, 2018). However, there are some unsolved questions about this genus. The validity of *Shaanbeikannemeyeria* was doubted. It has been proposed as synonymous with *Kannemeyeria* (King, 1988; Lucas, 2001), or congeneric with *Rechnisaurus* (Cox, 1991). Although the recent researchers have accepted its validity, no consensus has reached on its phylogenetic position. It was first proposed as the sister-taxon of *Kannemeyeria* (Kammerer et al., 2013), but recently has been viewed as an early diverged clade of Kannemeyeriiformes (Angielczyk et al., 2017; Kammerer et al., 2019; Kammerer and Ordoñez, 2021). The stratigraphical distribution of *Shaanbeikannemeyeria* also needs to be clarified.

During 1978–1980, teams from the IVPP collected three specimens of *Shaanbeikannemeyeria* from Fugu, Shaanxi and Junggar, Nei Mongol. In 1988 and 1997, more kannemeyeriiform specimens were collected by the teams led by Li Jin-Ling. These specimens are described here to clarify the distribution, the diagnosis, the variations, and the phylogenetic position of *Shaanbeikannemeyeria*. Moreover, the presence of the second dicynodont genus is confirmed from the lower Ermaying Formation.

2 Geological setting

The fossils were collected from a small area near the border between Shaanxi and Nei Mongol, corresponding to the Fugu County and Junger Banner respectively. Most specimens were collected from the lower Ermaying Formation, except one (IVPP V 11675) from the top of the Heshanggou Formation. A stratigraphic column was measured in 1997 and 1998 at Fugu, and the fossil horizons are marked (Fig. 1). The lower Ermaying Formation from Liulin, more than 200 km to the south, was dated as Anisian in age (Liu et al., 2018).

3 Materials

In addition to two holotypes of *Shaanbeikannemeyeria*, more kannemeyeriiform specimens were collected. Examined specimens are listed (Table 1). All listed specimens can be referred to *S. xilougouensis* except for IVPP V 30727 and V 30730, which are tentatively identified as *Parakannemeyeria*.

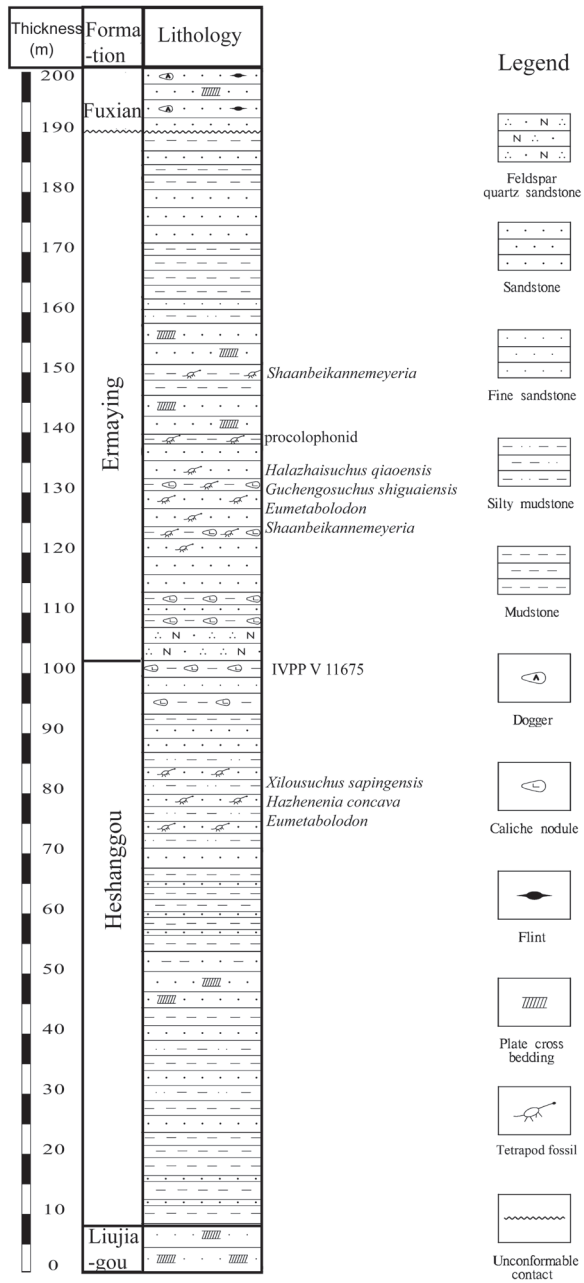

Fig. 1 Stratigraphic column of tetrapod fossil horizons in the studied area

Anatomical abbreviations acd, anterior condyle; act, acetabulum; An, angular; ap, anterior process; apr, anterior palatal ridge; Ar, articular; As, astragalus; Bo, basioccipital; bt, basal tuber; Ca, calcaneum; cap, capitulum; cen, centrum; cd, condyle; ch, choana; cnc, cnemial crest; co, crista oesophagea; cp, caniniform process; cr, cervical rib; D, dentary; d1–5, digital 1 to 5; do, dorsal opening of interpterygoid vacuity; dpc, deltopectoral crest; dr, dorsal rib; dt, distal tarsal; dv, dorsal vertebra; Ec, ectopterygoid; ect, ectepicondyle; ent, entepicondyle; entf, entepicondylar foramen; Ep, epipterygoid; epu, for epipubis; F, frontal; Fe, femur; Fi, fibula; fm, fenestra magnum; fo, fenestra ovalis; f.pap, facet for paroccipital process; f. qp, facet for quadrate ramus of pterygoid; f.s, facet for stapes; Hu, humerus; ic, internal carotid canal; IL, ilium; ipv, interpterygoid vacuity; Is, ischium; J, jugal; jf, jugular foramen; L, lacrimal; la, lacrimal foramen; ld, insertion of M. latissimus dorsi; lds, lateral dentary shelf; lf, labial fossa; lpf, lateral palatal foramen; M, maxilla; mf, mandibular fenestra; mpr, median palatal ridge; mt, metatarsal; n, naris; N, nasal; ns, neural spine; oc, occipital condyle; of, obturator foramen; olf, olecranal facet; P, parietal; pap, paroccipital process of opisthotic; Pbs, parabasisphenoid; pcd, posterior condyle; Pe,

periotic; Pf, prefrontal; pf, pineal foramen; Pl, palatine; Pm, premaxilla; Po, postorbital; Pop, postparietal; poz, postzygapophysis; Pp, preparietal; Pra, prearticular; prz, prezygapophysis; Pt, pterygoid; ptf, posttemporal fenestra; Pu, pubis; Q, quadrate; Qj, quadratojugal; qrp, quadrate ramus of pterygoid; Ra, radius; rl, reflected lamina of angular; Sa, surangular; scs, insertion of M. subcoracoscapularis; Sm, septomaxilla; So, supraoccipital; Sp, splenial; Sq, squamosal; sr, sacral rib; St, stapes; st, sella turcica; sup, supinator process; sv, sacral vertebra; T, tabular; t, tusk; Ti, tibia; tp, tympanic process; tr, trochlear; trm, trochanter major; u, ungual; Ul, ulna; V, vomer; wf, wear facet.

Table 1 List of studied specimens in this paper

	skull	skull basal length	lower jaw	postcranial bones
Shaanbeikannemeyeria				
adult				
IGCAGS V315[1)]	nearly complete	27 cm	absent	absent
IVPP V 6033[2)]	incomplete	31 cm	present	present
IVPP V 11674	nearly complete	24 cm	present	absent
IVPP V 11675	incomplete	~27 cm	present	absent
IVPP V 11677	incomplete	29 cm	present	absent
IVPP V 30728	absent		absent	left humerus
subadult				
IVPP V 11676	nearly complete	16 cm	present	scapula, humerus, clavicle
IVPP V 17904	incomplete	~21 cm	absent	absent
IVPP V 30725	incomplete	~14 cm	present	absent
IVPP V 30726	incomplete	~18 cm	present	nearly complete
juvenile				
IVPP V 30729*	incomplete	<10 cm	absent	absent
?*Parakannemeyeria*				
IVPP V 30727	absent		absent	partial skeleton
IVPP V 30730*	absent		absent	partial skeleton

Notes: 1) holotype of *S. xilougouensis*; 2) holotype of *S. buerdongia*; * found in association.

4 Systematic palaeontology

Anomodontia Owen, 1860

Dicynodontia Owen, 1860

Dicynodontoidea Olson, 1944

Kannemeyeriiformes Maisch, 2001

***Shaanbeikannemeyeria xilougouensis* Cheng 1980**

Holotype IGCAGS V315, a nearly complete skull.

Neotype IVPP V 11674, a nearly complete skull with lower jaw.

Type locality and horizon Xilougou, Gucheng Township, Fugu County, Shaanxi Province, China; base of Ermaying Formation.

Referred specimens IVPP V 6033, V 11676, V 11677, V 17904, V 30725, V 30726, V 30728, and V 30729, lower Ermaying Formation; V 11675, Heshanggou Formation.

Revised diagnoses Medium-sized kannemeyeriiforms with the following

autapomorphies: occiput strongly inclined relative to the palate such that the skull is much shorter basally than dorsally, sword tip-like premaxillary posterodorsal processes, tall and dorsally-convex cutting blade on medial edge of the dorsal surface of the dentary, reflected lamina with a separated posteroventral process, and 15 dorsal vertebrae.

Differentiated from *Uralokannemeyeria* by postorbital that does not extend the entire length of intertemporal bar, and an oblique ridge on lateral side of zygomatic arch in adults; differentiated from *Rechnisaurus* by lacking deep depressions lateral to the midline ridge on the snout; differentiated from *Kannemeyeria* by having the anterior tip of snout squared off, notch absent on the dorsal edge of narial opening, parietals exposed in the midline groove, and a median pterygoid plate with a thin median ridge on the ventral surface.

Differentiated from *Shansiodon* by its larger size, relatively small temporal fenestrae, intertemporal bar is wide, not crest-like and raised from the skull roof; differentiated from *Sinokannemeyeria* and *Parakannemeyeria* by short snout, premaxillary lateral surface anterior to the external naris without lateral extension, small caniniform process and tusk, narrower interorbital region, and longer intertemporal bar.

5 Description

The known specimens vary in their size (Supplementary file 1). The maximum known skull length (from the snout tip to the posterior edge of the squamosals) is 42 cm (holotype), and the maximum known occipital width is ~40 cm (holotype); while the smallest specimen is estimated to have a skull length of 12 cm (IVPP V 30729). The skull and lower jaw of each specimen are described separately, while the postcranial bones are described together. The skull of IGCAGS V315 and the lower jaw of IVPP V 11674 are described in detail, and other skulls and lower jaws only highlight some important similarities and differences between them.

5.1 Skull and lower jaw

IGCAGS V315 The skull is nearly complete, missing only the quadrate and quadratojugal complexes, and the left postorbital. No lower jaw is preserved. It was described and figured by Cheng (1980) (Fig. 2). This specimen was stored at IGCAGS; but it cannot be traced anymore. The following description is based on the observations before it was lost and the original description by Cheng (1980).

The skull is nearly triangular in dorsal view not accounting for the occiput. Its occiput is strongly inclined posteriorly such that the skull is much shorter basally than dorsally and relatively low. In lateral view, the skull anterior to the temporal fenestrae is strongly convex, with the peak on the nasals. The intertemporal bar extends posterodorsally, forming an angle of 120° with the frontal.

The premaxilla has a wide anterior surface which forms a nearly right angle with the lateral surfaces, giving the anterior tip of the snout a squared-off profile (Fig. 2). Posterodorsally, two premaxillae firstly substantially shrink in the width, then keep the width

for ~4 cm before finally rapidly converging at the midline such that they form sword tip-like processes between the nasals. The dorsal and lateral surfaces are covered by different-sized pits, indicating they were covered by the keratinous beak in life. The premaxilla has an obtuse anteroventral margin which nearly lies on a horizontal plane. Posteroventrally, the premaxillary ventral margin, together with the portion of the maxilla anterior to the caniniform process, forms a nearly straight cut-edge (Fig. 2C). On the palatal surface, the anterior ridges are paired and nearly parallel, and are also exposed in lateral view (Fig. 2B). Posterior to them, a middle ridge slightly increases in width posteriorly and meets the blade-like mid-ventral plate of the vomer at the anterior margin of the choanae.

The external naris is elongated and there is no distinct notch on the dorsal edge. The embayment lies mainly below the naris, and its postnarial portion is small. The external naris is surrounded by the premaxilla anteriorly, the nasal dorsally and the septomaxilla ventrally. The septomaxilla lies above the maxilla and within the embayment of the external naris.

On the dorsal surface, a distinct median ridge increases in width upwards and posteriorly from the ventral portion of the premaxilla to the anterior portion of the frontal. It measures 5 mm

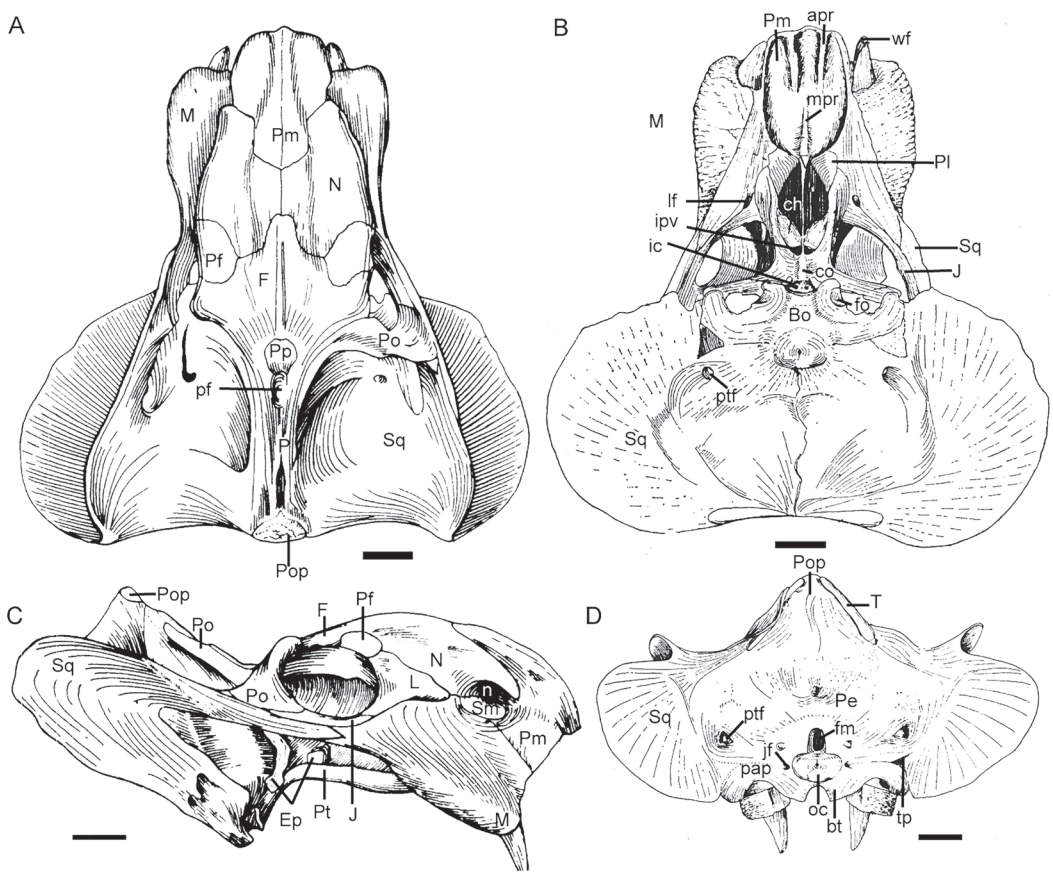

Fig. 2 Holotype of *Shaanbeikannemeyeria xilougouensis* (IGCAGS V315) from the Ermaying Formation, drawings of the skull in dorsal (A), ventral (B), lateral (C), and occipital (D) views
Revised from Cheng, 1980. Scale bars equal 4 cm

in width on the anterior tip, but 35 mm on the frontal. Posteriorly, it continues as a narrow low ridge on the frontal and disappears anterior to the prepariетal.

The maxilla has a short contact with the nasal dorsally and a straight suture with the premaxilla below the external naris. Posteriorly, it receives the anterior process of the squamosal laterally below the orbit and supports the jugal dorsally. The maxilla has a fat caniniform process, which lies slightly below the anterior extended line of the zygomatic arch and can be observed in dorsal view. The surface of caniniform process is rugose, but the above maxillary lateral surface is smooth. On the medial side, the caniniform process has a clear oblique furrow with the smooth maxillary palatal surface. Medial to this margin, a large labial fossa is formed by the maxilla, jugal and palatine. The exposed tusks are short (47 mm) with sharp tips that are pointed anteroventrally. The tusk has a smooth wear facet on the medial side. The distance between the two tusks is 65 mm.

Two nasals occupy the largest area on the dorsal surface. It has a short posteromedial margin for the anteromedial process of the frontal and meets the counterpart on the midline. Its surface is rough, especially on the posterolateral side. The nasal boss is absent.

The ovoid orbit faces mainly laterally, but also slightly anteriorly and dorsally. It is formed by the prefrontal and frontal dorsally, the lacrimal anteriorly, the postorbital posteriorly, and the jugal ventrally. The jugal forms the major part of the zygomatic arch, but it has a narrow lateral exposure. On ventral side, it extends anteromedially to contribute to the margin of the labial fossa. The zygomatic arch is robust and its anterior (orbital) portion is rod-like. The posterior portion is transversely expanded and has an oblique ridge on lateral side, so it is triangular in cross-section.

The triangular lacrimal is exposed anterior to the orbit on the lateral surface. Its anterior tip is close to but does not reach the septomaxilla. The rounded lacrimal foramen lies in a deeply concave area of the posterior ventral side of the bone. Above it lie a few narrow ridges. The lacrimal bulges laterally related to the maxilla. It has a triangular ventral process overlapping the anterior process of the jugal on the orbital ventral margin.

The small prefrontal lies on the anterodorsal corner of the orbit and is mainly exposed on the dorsal surface. It extends only slightly beyond the orbital anterior margin and nearly lines with the anterior extension of the frontal, but it is far behind the anterior extension of the lacrimal. Its suture with the lacrimal is unclear, but it is separated from the maxilla.

The two frontals have smooth surfaces and meet with a thin and low mid-ridge. Anteriorly, their short anteromedial processes insert between the nasals, while posteriorly, they surround the prepariетal and meet at the parietal. The frontal forms half of the orbital dorsal margin.

The postorbital forms the posterior margin of the orbit, the entire anterior margin, and most of the medial margin of the temporal fenestra. Its anterior portion is a wide strip which expands ventrally and overlaps the jugal laterally. It does not extend to the entire length of intertemporal bar posteriorly, and the posterior portion of the intertemporal bar is formed only by the parietals.

The preparietal lies on the concave area anterior to the pineal foramen and forms the anterior wall of the latter. The oval pineal foramen is a large, deep, dorsal opening.

The parietals are well exposed on the intertemporal bar and raised as a nearly straight crest, similar to *Rhadiodromus* (Surkov, 2003). Two parietals meet along the midline to form a shallow groove. Posteriorly, they are separated by the postparietal on the skull roof and contact the squamosal laterally. The parietal and postorbital do not form fossa on the ventral surface of the intertemporal bar.

The large temporal fenestra is widened posteriorly. The squamosal constitutes the lateral and posterior margins of the temporal fenestra. It sends a long zygomatic process to contact the maxilla anterior to the postorbital bar (Fig. 2C). Its zygomatic process decreases the height posterior to the postorbital bar, and attenuates into a slice on the base in the lateral view, but it flares posteriorly with a wide base in dorsal view. In posterior view, the squamosal margin forms a distinct dorsolateral notch below the zygomatic arch (Fig. 2D). The squamosal distinctly extends laterally, forming the lateral portion of the occiput. Dorsomedially, it contacts the parietal and the postorbital on the anterior surface of the occiput, the tabular and the periotic on the posterior surface of the occiput. It contributes to the lateral margin of the posttemporal fenestra. Anteroventrally, it has a pocket for receiving the quadrate and quadratojugal.

The vomer forms a vertical thin plate behind the median palatal ridge of the premaxilla and divides the choanae from the middle. Its posterior border with the palatines and pterygoid is unclear.

The palatines flush with surrounding palatal elements. Its rugose anterior pad sutures with the posteromedial process of the premaxilla, and separates the maxilla from the border of the choana. Its laminar posterior portion is smooth and forms the medial side of the lateral wall of the choana. Two palatines are separated by the vomer. No ectopterygoid is visible on this specimen.

The pterygoids have the typical ‘X’-shape as in all dicynodonts. The robust anterior pterygoid rami are elongated and contact the maxilla. Their anterior tips are narrow ventrally as keels (the anterior pterygoid keels), and the ventral ridge on the posterior portion is indistinct and merges to the smooth median pterygoid plate. The median pterygoid plate is transversely wide, with a low crista oesophagea on the ventral surface. The oblate interpterygoid vacuity is short but wide and opens anteroventrally. The quadrate rami are thin, ribbon-like structures without twists and are directed more laterally than posteriorly (two rami forming an angle of ~120°).

The right epipterygoid is preserved. It is like a curved strap resting on the top of the pterygoid. Its footplate extends from the quadrate rami to the lateral of the medial plate, the ascending process contacts the parietal, and the short anterior process is partially preserved above the pterygoid (Fig. 2C).

The parabasisphenoid expands posteriorly and forms two lateral ridges. Medial to the ridges, lie the paired, ventrally-directed openings of the internal carotid canals. The posterior portion of the bone turns ventrally and forms the anterior surface of the basal tubera. The

parabasisphenoid bears an elongate cultriform process anteriorly, which is damaged but can be seen through the interpterygoid vacuity in ventral view.

The basioccipital forms the major portion of the basal tubera, which is strongly rounded and the anterior and posterior tips of tuber curve towards each other and nearly enclose the fenestra ovalis. The basal tuber is inflated, and extends ventrally far beyond the palate. The intertuberal region is smooth, U-shaped, and without an intertuberal ridge.

Two strips on the dorsal margin of the occiput are identified as the relict of the tabular by Cheng (1980). They do not extend onto the dorsal surface of the intertemporal bar and cannot be observed in dorsal view. The postparietal is mainly exposed on the occiput, although it also has a small exposure on the intertemporal skull roof. It is curved posterolaterally and forms a concave area on the top of the occiput (Fig. 2D). Its ventral and lateral borders are unclear, but it looks like it is separated from the squamosal by the tabular.

Below the postparietal, the supraoccipital forms the dorsal margin of the foramen magnum. No distinct suture is observed between the supraoccipital, exoccipitals, opisthotics, and basioccipital, and these elements are fused as a single periotic element as in many dicynodonts (Kammerer et al., 2019; Liu, 2021). The foramen magnum is small and nearly square and lies ventrally on the occiput. Lateral to the foramen magnum and above the occipital condyle, lie two knoblike processes, for the articulation to the proatlases. The small occipital condyle is subspherical in posterior view. A circular central depression presents on the occipital condyle. The ovoid jugular foramen, lateral to the occipital condyle, is the passage for the glossopharyngeal (IX), vagus (X), and spinal accessory (XI) nerves as well as the internal jugular vein.

The paroccipital process is almost laterally directed. Its lateral edge, which sutures to the squamosal, draws into a posteriorly-directed process for the dorsal portion, similar to the tympanic process of Dicynodontoides (Cox, 1959). On its dorsolateral surface, a depression accommodates the posterolaterally directed posttemporal fenestra. The small posttemporal fenestra lies at the level of the top of the foramen magnum.

IVPP V 11674 The skull is nearly complete, except that the left caniniform process and tusk, the pterygoids, and the parabasisphenoid are incomplete, and the stapes and quadrates are missing. It is the best-preserved skull out of the available specimens. It is slightly shorter than the holotype, its occiput is not as expanded as in the holotype (Fig. 3), and the occipital width is less than the dorsal length of the skull (Supplementary file 1).

The caniniform process is slightly ventral to the anterior extended line of the zygomatic arch, and the tusk lies on the medial margin of the caniniform process. The tusk is longer and more robust than in the holotype. The exposed length of the right tusk is 65 mm. The base of tusk has an elliptic cross-section, measuring 24 mm at the greatest diameter. The wear facets lie on both the anterolateral side and medial side, and the anterolateral one is smaller but deeper. The striations are clearer and denser near the tip, mainly arranging in the direction of long axial of the tusk. The right tusk is formed by four distinct layers, possibly related to its age.

The snout tip is sharper than in the holotype (Figs. 2, 3). The premaxillae have sword tip-like posterodorsal processes. The frontal has an anteromedial process which approaches the premaxilla. The narrow intertemporal bar forms an angle of 135º with the frontal in lateral view (Fig. 4). A midline parietal ridge lies posterior to the pineal foramen. Although the quadrate is lost, the dorsal process of the right quadratojugal still rests on the fossa of the squamosal.

The lacrimal does not extend anteriorly as far as in the holotype. The prefrontal has distinct ridges and furrows on the lateral surface. The zygomatic arch is nearly flat dorsoventrally for the orbital portion (Fig. 4A).

Posterior to the palatine pad, the elongate lateral palatal foramen lies between the palatine and the anterior ramus of the pterygoid. The ectopterygoid has a clear suture with the pterygoid, it extends anteriorly beyond the anterior pterygoid ramus. This bone is fused

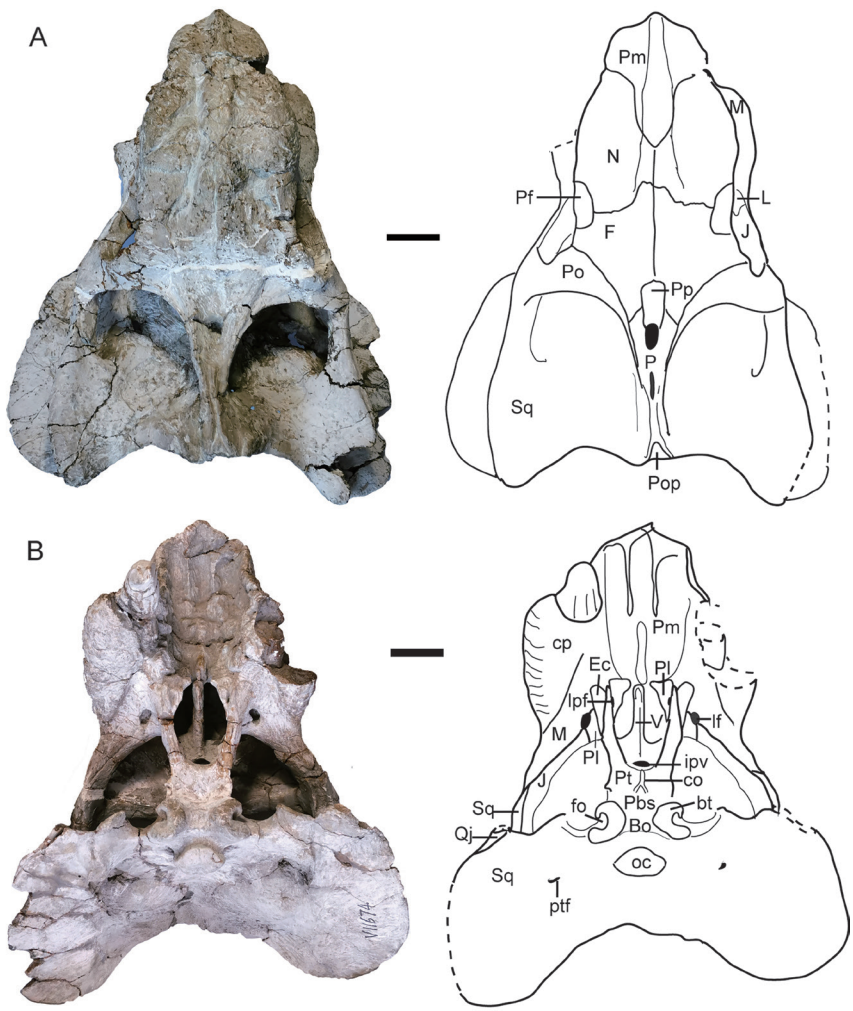

Fig. 3 *Shaanbeikannemeyeria xilougouensis* from the Ermaying Formation (IVPP V 11674), skull: photos and interpretive drawings in dorsal (A) and ventral (B) views. Scale bars equal 4 cm

to the pterygoid in the holotype, possibly for the later ontogenetic stage. The labial fossa is bordered by the maxilla laterally and the palatine medially, while the jugal only contributes a small portion of its posterior border. The interpterygoid vacuity is short but wide and opens anteroventrally. The pterygoid quadrate processes are missing. The parabasisphenoid is strongly curved ventrally, and the basal tubera is inflated.

The dorsal margin of the occiput extends only slightly dorsal to the squamosals (Fig. 4B) and is less developed than in the holotype. It is unclear if the tabular is present. The upper margin of the supraoccipital can be demarcated by the bulge of bone, forming a pair of 'wings'.

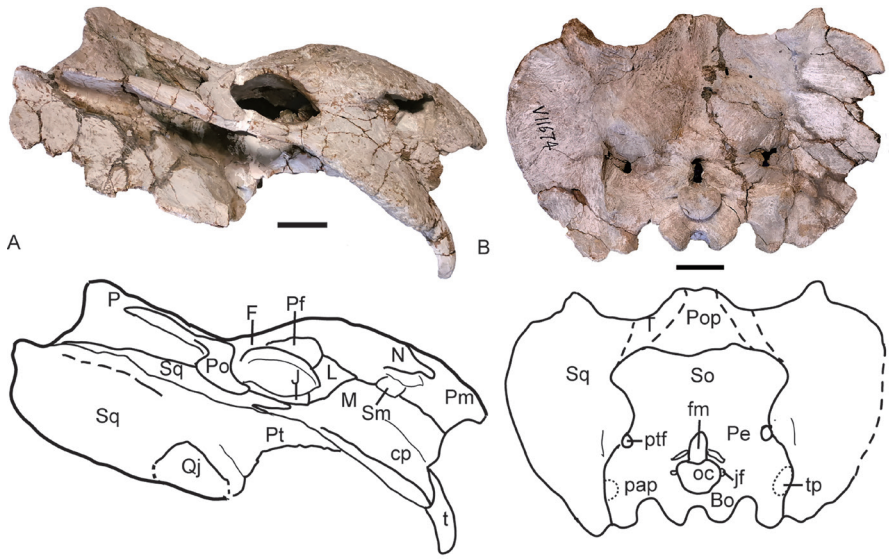

Fig. 4 Photos and interpretive drawings of the skull of *Shaanbeikannemeyeria xilougouensis* (IVPP V 11674) in right lateral (A) and occipital (B) views
Scale bars equal 4 cm

The lower jaw is almost complete except for the anterior margin of the dentary symphysis (Fig. 5). It is short (18 cm), only about half of the skull length.

The dentary symphysis is anteroposteriorly short but dorsoventrally tall and nearly square-shaped in dorsal view. The symphysis is thickened anteroventrally. There is no distinct ridge on the edge between the anterior and lateral dentary surfaces. The anterior and lateral surfaces of the dentary symphysis are rugose, while the dentary lateral surface is smooth above the mandibular fenestra. The dentary dorsal margin forms two sharp ridges, of which the medial one is taller and forms a dorsally-convex blade (Fig. 5B). On the dentary table, the area between the two ridges is slightly concave. Posteriorly, it develops as a distinct posterior dentary sulcus.

Posteriorly, the dentary sends two rami, the longer dorsal one forms the dorsal margin of the mandibular fenestra and contacts the surangular, the ventral one is a triangular process lateral to the angular. The lateral dentary shelf increases in height anteriorly from a small ridge above the mandibular fenestra.

The splenial is fused in the symphysis and its anterior process is exposed in ventral view. Along the midline, there are two fossae: the shallow one between the dentary and splenial and the deep one within the splenial. The splenial has no lateral exposure. It partially covers the angular medially and is covered by the prearticular laterally.

The angular is the second largest bone in the lower jaw. Anterolaterally, it has a trough for receiving the posterior process of the dentary. In lateral view, it bifurcates into two rami by the trough: the short anterodorsal ramus is triangular, extending to the anterior margin of the mandibular fenestra, and the long anteroventral ramus inserts between the dentary and the splenial and contributes to the symphysis. Posteriorly, the angular bears a large and rounded reflected lamina which is widely separated from the articular. Ventral to the lamina, there is a small posteroventrally-directed process which should be part of the reflected lamina but is separated from the main body by a deep notch. Medially to the reflected lamina, the angular contacts the articular posteriorly and the surangular posterodorsally. It is covered by the prearticular medially.

The surangular lies between the dentary and the articular, and is partially covered by the prearticular medially. The prearticular is a long strip-like bone, which completely covers the

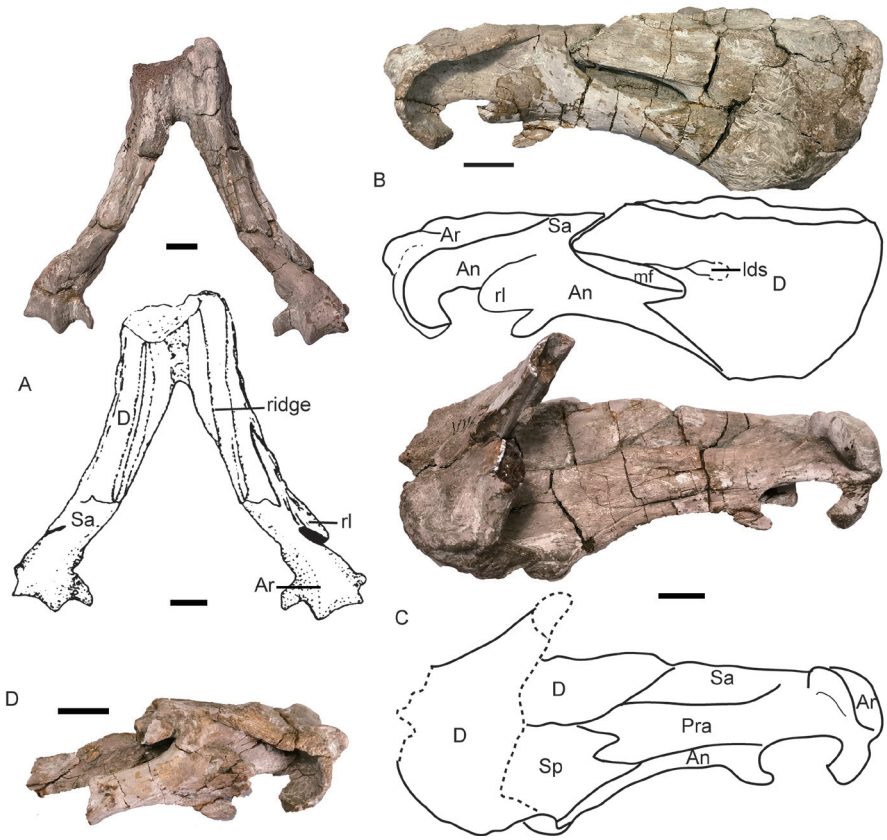

Fig. 5 *Shaanbeikannemeyeria xilougouensis* (IVPP V 11674), lower jaw, photo and interpretive drawing in dorsal (A), right lateral (B), and right medial (C) views; posterior portion of left ramus in lateral view (D) Scale bars equal 2 cm

mandibular fenestra medially. Posteriorly it is partially fused to the articular. The articular has a short anterior process extending between the prearticular and surangular. The lateral condyle is much wider than the medial one. It has a well-developed retroarticular process that curves forward.

IVPP V 6033 The dorsal portion of the skull was eroded, and only the palate and occiput are preserved with the lower jaw (Fig. 6). It is similar to IGCAGS V315 in size but the occiput is less inclined, so it has the greatest basal length (31 cm). Its occiput has a height which is slightly greater than half of the width as in IGCAGS V315, but the skull maximum length is smaller than the latter.

The caniniform process is incomplete but similar to the previous specimens. The tusk is similar in size to that of IVPP V 11674, but the distance between the two tusks (9 cm) is wider. The zygomatic arch has flat dorsal and ventral surfaces. The two sides are less convergent as in previous specimens, forming an angle of ~35°. In IGCAGS V315 and IVPP V 11674, this angle is greater than 45°. The temporal fenestra also has a length greater than the width.

On palate, the interpterygoid vacuity is relatively small and lies dorsal to the anterior margin of the medial pterygoid palate. The parabasisphenoid is strongly curved ventrally and attached to the anterior side of the basal tuber. No tabular can be identified on the occiput. The occipital condyle is bigger than that of IGCAGS V315 and the fenestra magnum looks wider as well.

The lower jaw is nearly complete, but it is occluded with the skull. It has a length of 20 cm, about half of the skull's dorsal length. It is similar to the lower jaw of V 11674 in shape.

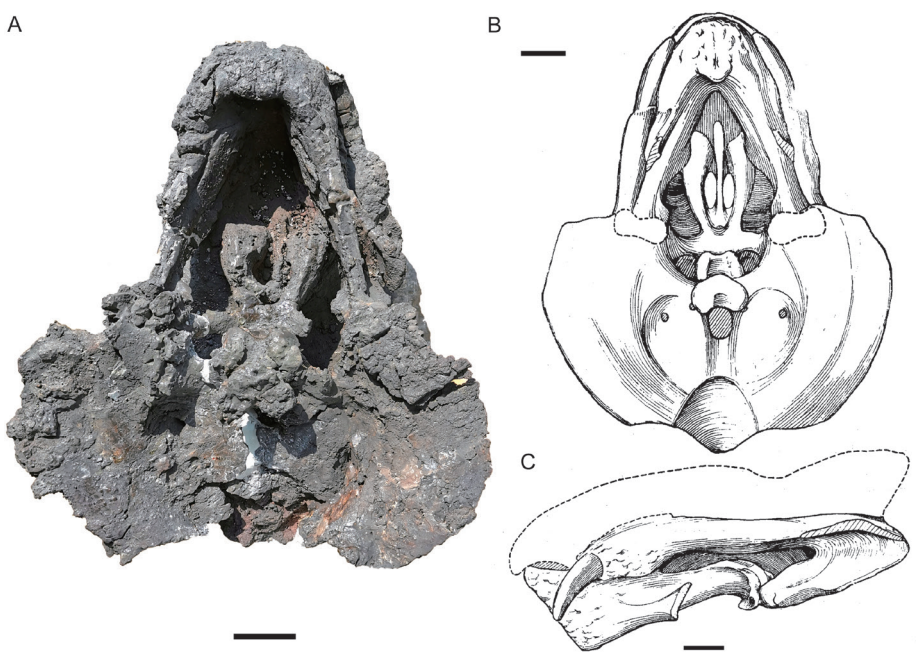

Fig. 6 Holotype of *Shaanbeikannemeyeria buerdongia* (IVPP V 6033) from the Ermaying Formation
Skull with lower jaw: photo (A) and interpretive drawing (B) in ventral view,
drawing (C) in left lateral view (drawing revised from Li, 1980). Scale bars equal 4 cm

The reflected lamina of the left angular diverges laterally near the middle of the lower jaw, and the ventral portion of the angular was eroded.

This specimen was compared with the holotype of *S. xilougouensis*, and the following differences were proposed (Li, 1980): narrower skull with occipital width around 3/4 skull length; snout tip obtuse and wider; bigger occipital condyle and foramen magnum; poorly developed caniniform process; longer and stouter tusks which are wider spaced; zygomatic arch nearly flat dorsoventrally.

IVPP V 11677 This specimen preserved like IVPP V 6033: the dorsal surface was eroded, and the lower jaw is occluded with the skull (Fig. 7). It is slightly smaller than V 6033.

It has the largest known tusks, and the tusks are spaced with 10 cm distance between them at the roots. The right tusk bears a wear facet on the anterolateral side, which is 40 mm

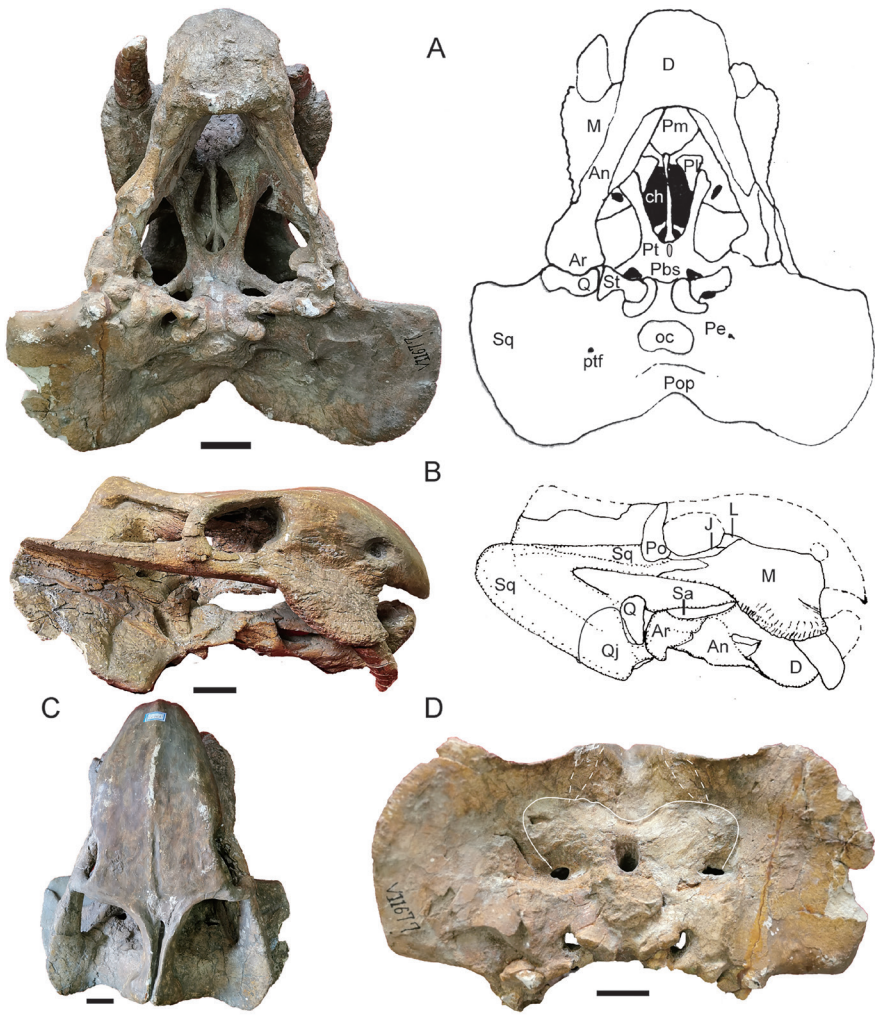

Fig. 7 Photos and drawings of the skull with lower jaw of *Shaanbeikannemeyeria xilougouensis* from the Ermaying Formation (IVPP V 11677)

A. ventral view; B. right lateral view; C. dorsal view; D. occipital view. Scale bars equal 4 cm

in length, and the striations in axial direction are dense near the tip. It also bears a less distinct facet on the medial side. The caniniform process is robust to contain the large tusk. The medial border of the rough area is curved and not straight as in the holotype. The labial fossa is quite large.

The zygomatic arch below the orbit is rod-like. Two sides also form a small angle as in V 6033 and are less convergent than as in IGCAGS V315 and V 11674. The maxillary zygomatic process extends posteriorly to the level of the anterior margin of the postorbital, slightly further than in other specimens.

The median pterygoid plate has a low and wide crista oesophagea. Two quadrate rami are slender, forming an angle of ~120º. Its tip inserts into the quadrate, the stapes, and the paroccipital process of the periotic. The interpterygoid vacuity is sub-triangular and opens ventrally. Its anterior margin lies anterior to the medial pterygoid plate. The parabasisphenoid runs dorsally across it and divides it into two openings. The parabasisphenoid is slightly curved ventrally, but not as strong as in previous specimens. The epipterygoid is preserved in the dorsal process on the right side.

The quadratojugal is fused to the dorsal surface of the quadrate lateral condyle, and two bones form a quadrate-quadratojugal complex. The quadratojugal dorsal process is fan-like within the shallow squamosal lateral pocket, and its dorsal margin loosely connects with the squamosal. The quadrate dorsal process is smaller than that of the quadratojugal. The right quadrate condyles are exposed in ventral view because the articulated lower jaw slid upwards (Fig. 7A). The lateral surface of the median condyle is attached by the stapes on the ventral flange and by the pterygoid quadrate process and the paroccipital process on the dorsal concave area.

Both stapes are preserved in situ. It is a column-like bone with constricted waist. Its medial surface articulates to the fenestra ovalis, and the lateral surface, which is larger, articulates to the quadrate. The occiput is quite wide, with a rectangular-shape (Fig. 7D). The occipital condyle is relatively big. The foramen magnum has a width subequal to the height.

The lower jaw is estimated to be 20 cm in length including the missing dentary tip. The symphysis is robust and high, with a length of 7 cm. A middle ridge develops on the dentary anterior surface, and it widens and decreases in height ventrally. The reflected lamina of the angular is incomplete on either side, but it preserved a ventrally directed portion, although it is unknown if it is a separated process as in V 11674.

IVPP V 11675 The dorsal portion of skull is almost fully eroded, except for the bone around the pineal foramen (Fig. 8). The right lateral side and the palate are relatively complete. The skull has a width of ~36 cm and a basal length of ~27 cm. The tusk is short but bulky, with a diameter of 26 mm and exposed length of 55 mm. The caniniform process is rounded, and the tusk lies on its medial side. It also lies slightly below the anterior extension line of the zygomatic arch.

The right zygomatic arch is complete, and its orbital portion is rod-like. Two zygomatic arches form a big angle (59º). The maxilla extends posteriorly to the level of the anterior

margin of the postorbital. The squamosal extends anteriorly beyond half of the orbital ventral length. The oval pineal foramen is quite large (Fig. 8D). The lingulate preparietal lies on the concave area anterior to the pineal foramen and forms the anterior wall of the latter. The preserved intertemporal bar is same as in other specimens.

The interpterygoid vacuity lies far anterior to the median pterygoid plate, and it is longer than it is wide. Its dorsal openings are small (Fig. 9). The crista oesophagea is a low ridge on the median pterygoid plate. The parabasisphenoid is nearly flat, only the two posterolateral corners curve to an angle of ~30º and form a small portion of the basal tubers. The openings for the internal carotid canal are not so clear on the ventral surface, but the dorsal openings sit deeply within a triangular pyramid-shaped sella turcica, which houses the pituitary gland. The sella turcica is formed only by the parasphenoid.

The right squamosal is nearly complete. The occiput is relatively low and the occipital height is about half of its reconstructed width. The occiput is strongly inclined posteriorly. The occipital condyle is semicircular with concave dorsal surface. The right quadrate-quadratojugal

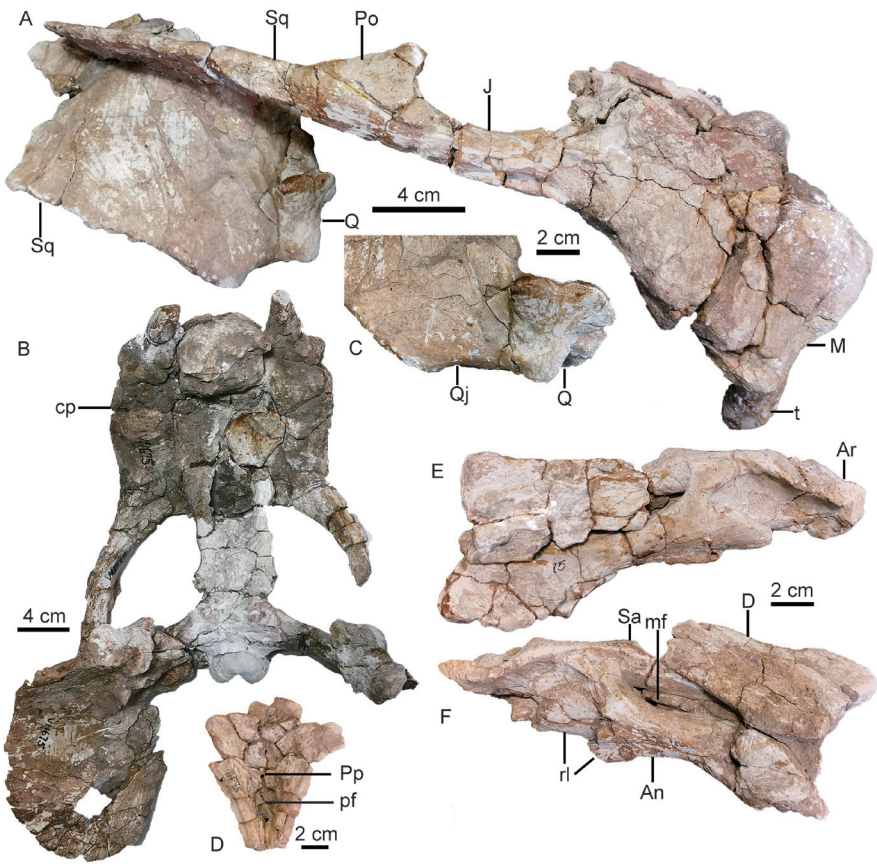

Fig. 8 *Shaanbeikannemeyeria xilougouensis* from the Heshanggou Formation (IVPP V 11675)
A, B. skull in lateral (A) and ventral (B) views; C. quadrate and quadratojugal in anterolateral view;
D. the region around the parietal foramen inn dorsal view;
E, F. lower jaw, part of the left ramus (E) and the right ramus (F) in lateral view

complex is preserved in the anteroventral pockets of the squamosal, and the fan-like dorsal process of quadratojugal is firmly sutured with the squamosal (Fig. 8C).

The absolute size of the lower jaw is bigger than that of V 11674. The robust symphysis is occluded with the snout (Fig. 8B). The vertical portion of the reflected lamina is present, but it is unknown if it is a separate process (Fig. 8E, F).

IVPP V 17904 The skull was sheared and skews to the right side (Fig. 10). The posterior portion including the occiput is not preserved. This skull is smaller than that of V 11674, with an estimated base length of 21 cm. The caniniform process is only weakly developed. The tusk is short and thin. The zygomatic arch is curved laterally and the orbit can be partially observed dorsally, similar to V 11674.

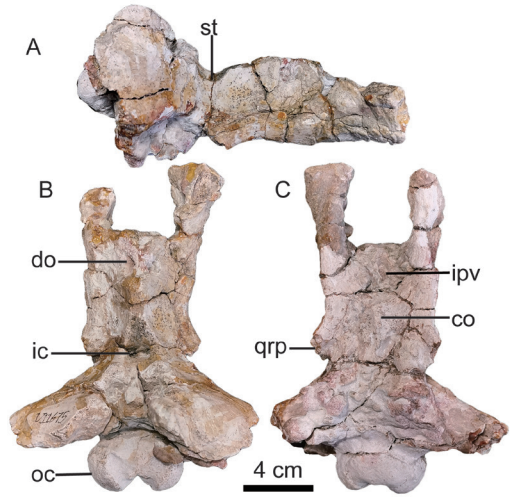

Fig. 9 Ventral-posterior portion of skull of *Shaanbeikannemeyeria xilougouensis* from the Heshanggou Formation (IVPP V 11675) in right lateral (A), dorsal (B) and ventral (C) views

The labial fossa is small and rounded, and most of the posterior margin is formed by the jugal, but the posteolateral side is covered by the maxilla if it is complete (Fig. 10B). The median pterygoid plate has no distinct ridge, but a suture on that position indicates the unfused pterygoids. The interpterygoid vacuity is round and opens ventrally. It is almost covered dorsally by the parabasisphenoid, and only a small opening presents on the left side.

The parabasisphenoid expands posteriorly and forms two lateral ridges. Medial to the ridges, paired depressions lie on the anterior portion of the parabasisphenoid. Posteriorly to the shallow depressions, the paired ventrally-directed openings of the internal carotid canals lie on the narrowest part of the parabasisphenoid. The basal tubera are not so well developed and the groove between them is shallow.

IVPP V 11676 The skull measures 16 cm in basal length (Fig. 11). It has undergone anteroposterior compression and there are many cracks. There is no distinct midline ridge on the dorsal surface of the snout. The premaxillae have the same sword tip-shaped posterodorsal processes as in the holotype. The frontal anteromedial processes approach the premaxilla, and the nasals are nearly divided by them. The small prefrontal is nearly semicircular and only forms a small portion of the orbital dorsal margin. The preparietal is almond-like, lying at the level of the postorbital bars. The intertemporal bar is relatively wider compared to larger specimens. The postorbitals form the lateral ridges of the intertemporal bar, bracing a concave area formed by the parietals. A weak protuberance lies along the axial line posterior to the pineal foramen as in V 11674.

The caniniform process is less developed and the rough area is narrower than in the large specimens (Fig. 11). The tusks are small and short. The triangular lacrimal bulges laterally

and approaches the septomaxilla. The small lacrimal foramen lies within the middle of the orbital anterior wall. The zygomatic arches are convex laterally, so the orbits open somewhat dorsally. The orbital portion is more or less rod-like. The orbit has large exposure in dorsal view. The intertemporal bar is slightly convex dorsally, and forms an angle of 130º with the frontal in lateral view. The postparietal has a small exposure on the skull roof. Both sides of the quadrate-quadratojugal complex are preserved, although the right one is partially detached from the skull (Fig. 11E, F).

The palate is poorly preserved and no clear sutures are visible (Fig. 11C). The labial fossa is small. The skull is broken along the parabasisphenoid as in V 11674. It seems the medial pterygoid plate was pushed upwards compared to the basal tuber by compression.

The occiput is relatively high (Fig. 11D), the ratio of occipital height to occipital width

Fig. 10 Skull of *Shaanbeikannemeyeria xilougouensis* from the Ermaying Formation (IVPP V 17904) in dorsal (A), ventral (B), and right lateral (C) views
Scale bars equal 4 cm

is 0.79, slightly smaller than that of the holotype (0.82) and V 11674 (0.84), much greater than in V 6033 (0.62) and V 11677 (0.65). The foramen magnum is rounded. The posttemporal fenestra is small. The occipital condyle is damaged but should be tri-radiate in posterior view.

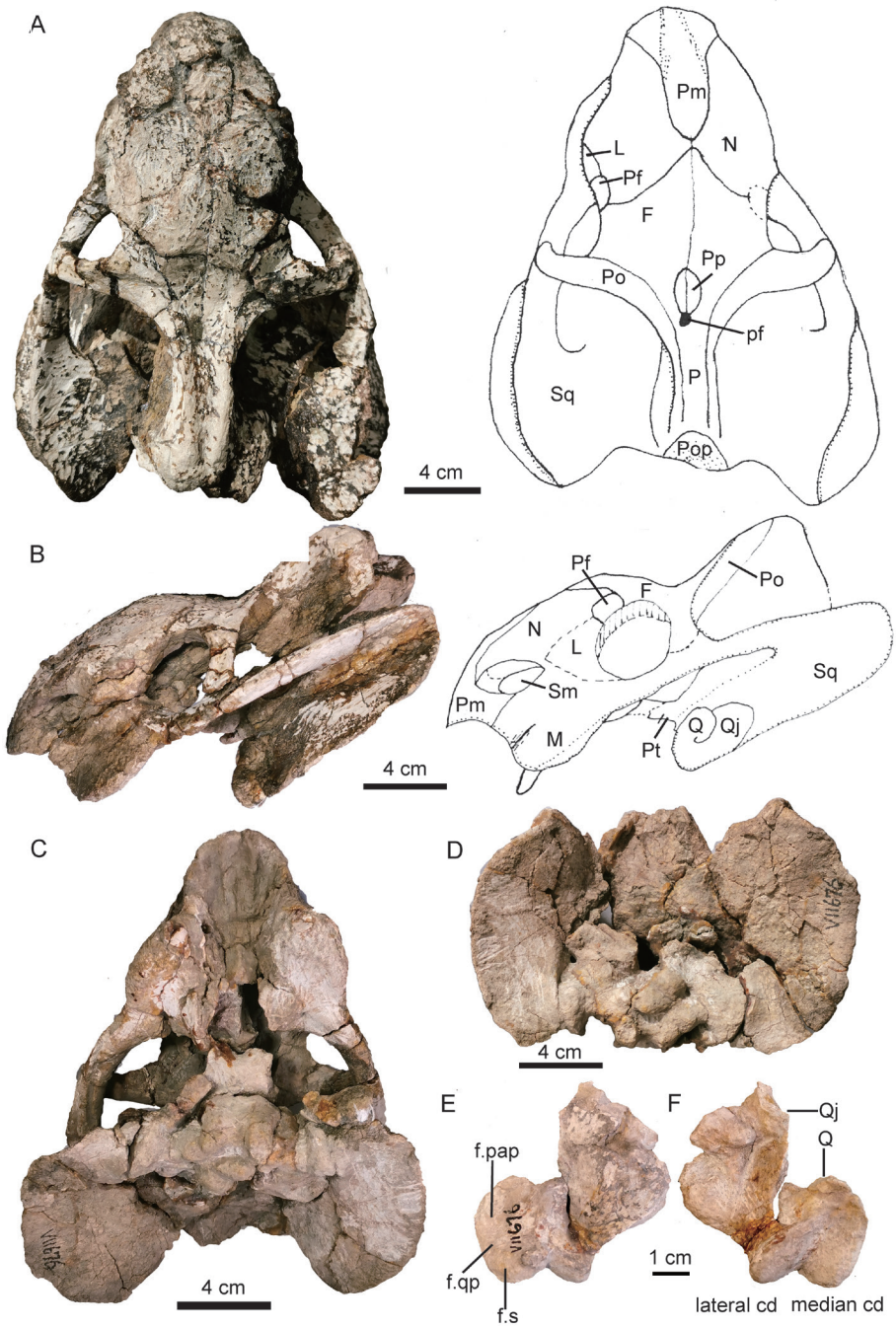

Fig. 11 *Shaanbeikannemeyeria xilougouensis* from the Ermaying Formation (IVPP V 11676) Photos and interpretive drawings of the skull in dorsal (A), right lateral (B), ventral (C) and occipital (D) views; left quadrate and quadratojugal complex in anterior (E) and posterior (F) views

The basic pattern of the lower jaw is the same as in V 11674 (Fig. 12). The symphysis is complete in this specimen, and its dorsal margin is distinctly curved dorsally, higher than the dentary rami. A low midline ridge is present on the anterior surface of the symphysis and disappears below at half the height. On the dorsal margin of the dentary, the medial edge forms a dorsally-convex cutting blade (Fig. 12C). Although the reflected lamina is incomplete, it has a remnant of vertical ventral portion on the right side which is clearly separated from the upper portion (Fig. 12B). It indicates that this portion could be the same as that of V 11674. The reflected lamina is far from the articular.

IVPP V 30725 The skull is heavily eroded with only two caniniform processes, the zygomatic arches, the posterior portion of the skull roof, and the middle portion of the palate are preserved, while the lower jaw is almost complete (Fig. 13). The skull dorsal length is estimated as ~18 cm.

The flat caniniform process wraps the lateral side of the tusk. The maxilla extends posteriorly only to the middle of the orbit. The orbital portion of the zygomatic arch is dorsoventrally flat. The interpterygoid vacuity is round and opens ventrally. The quadrate rami form an angle of 115º. The lower jaw is 11 cm in length. The reflected lamina is incomplete.

IVPP V 30729 Most of the dorsal and right lateral side of the skull is preserved (Fig. 14). The preserved skull length is 10 cm, and it is estimated with a dorsal length of 12 cm. This specimen is the smallest among known specimens and is likely a juvenile.

The premaxillae are unfused. They have slender posterodorsal processes, and the

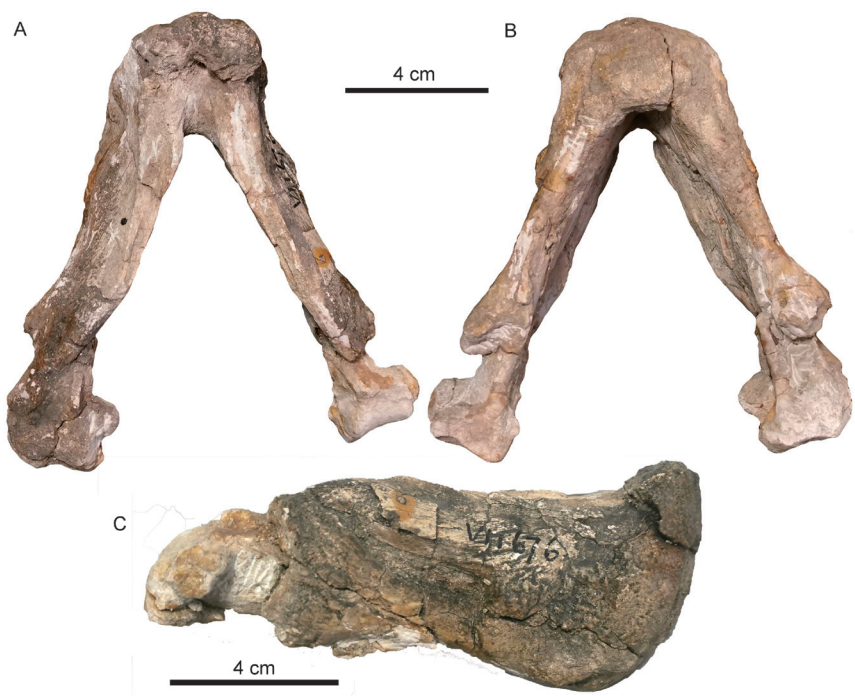

Fig. 12 *Shaanbeikannemeyeria xilougouensis* from the Ermaying Formation (IVPP V 11676), lower jaw in dorsal (A), ventral (B) and right lateral (C) views

posterolateral margins are formed by one straight line rather than two segments as in other specimens. The maxilla has a poorly developed and broken caniniform process, which lies slightly below the anterior extended line of the zygomatic arch. The frontal anteromedial processes form a sharp angle and nearly touch the premaxillae. The prefrontal is relatively small, while the lacrimal is a large element forming the anterior orbital wall. The small lacrimal foramen lies in the middle of the anterior orbital wall. The lacrimal send a triangular process to cover the jugal dorsally. The maxilla sends a long posterior process which contacts the squamosal laterally, and the posterior end inserts between the squamosal and the jugal on the ventral surface of the zygomatic arch and extends to the level of the anteroventral margin of the postorbital.

IVPP V 30726 Only the palate of the skull is preserved and exposed in dorsal view (Fig. 15A). The lower jaw is articulated to the skull. Two quadrate rami form an angle of 120º. The exposed braincase has a rounded fossa, which is formed by the parabasisphenoid anteriorly, the exoccipitals posteriorly, and the prootic and opisthotic laterally. The sutures are still identifiable, indicating a young stage of the individual. It seems only the left ramus of the lower jaw is preserved and partially exposed in dorsal view. The identification of this specimen is mainly based on postcranial bones.

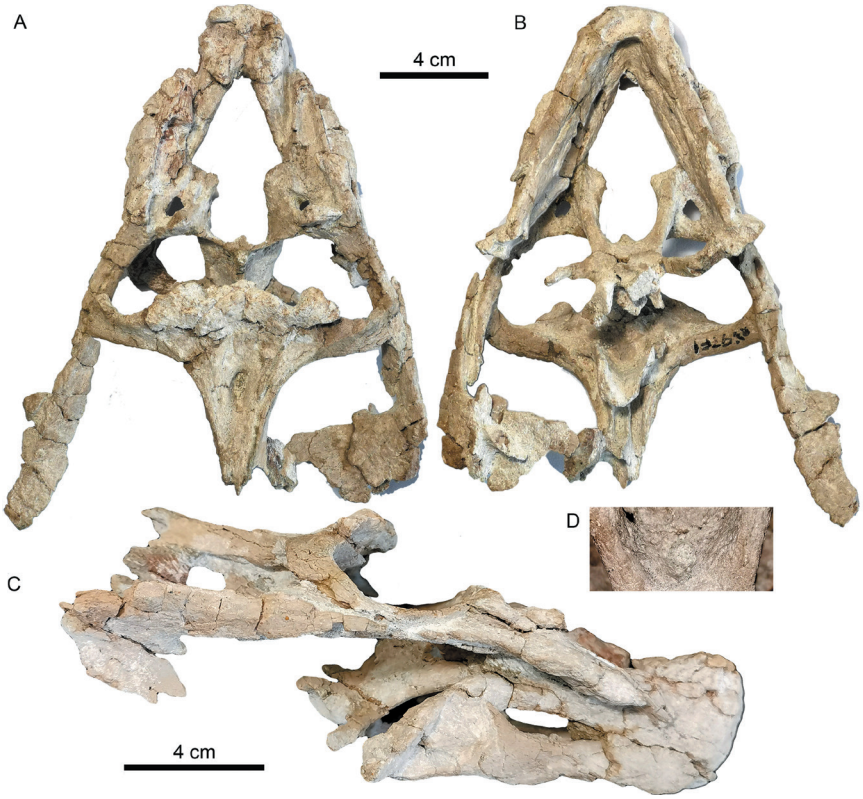

Fig. 13 *Shaanbeikannemeyeria xilougouensis* from the Ermaying Formation (IVPP V 30725) Incomplete skull with lower jaw in dorsal (A), ventral (B), and right lateral (C) views; part of the pterygoid showing the interpterygoid vacuity (D)

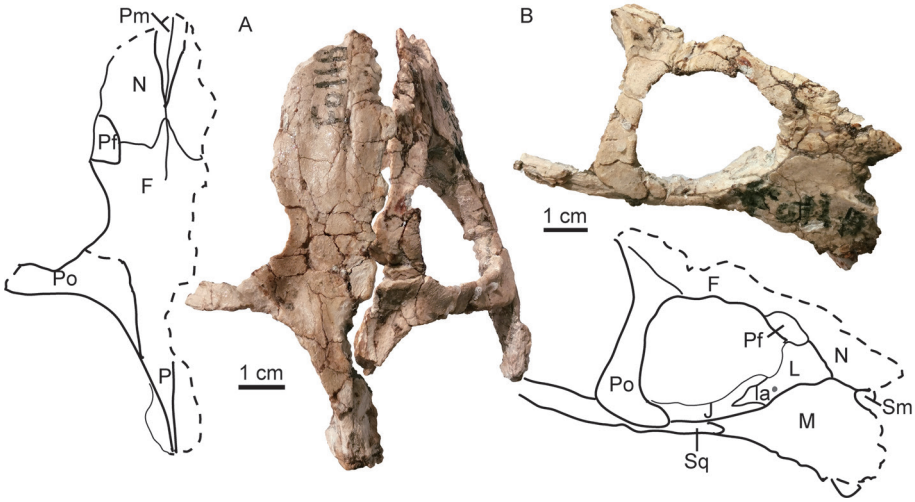

Fig. 14 Photos and interpretive drawings of the Skull of *Shaanbeikannemeyeria xilougouensis* from the Ermaying Formation (IVPP V 30729)
A. left portion in dorsal view; B. right portion in lateral and slightly dorsal view

5.2 Postcranial skeleton

The postcranial elements of *Shaanbeikannemeyeria* are preserved in IVPP V 6033, V 11676, V 30726, and possibly in V 30728. The postcranial skeleton is nearly complete in V 30726, but the bones are not in a good state and the preparation is incomplete. The description of vertebrae and ribs is based on V 30726.

Axial skeleton Most cervical vertebrae are not exposed except for the neural spines of the last few. However, their number can be counted based on the articulating ribs (Fig. 15B). The first preserved rib is a real short one (< 2 cm) and close to the head, it should belong to axis. The following ribs have a wide head and the capitulum and tuberculum can be identified, but there is no distinct groove separated them. The 7th rib is similar to the 6th rib in shape but is identified as the first dorsal for its position and the first dorsal is similar to last cervical in many dicynodonts (Sun, 1963; Bandyopadhyay, 1988; Liu, 2021). The dorsal number is counted as 15 as shown in Fig. 15. The sacral region is not so well preserved, but the number should be no less than 5 based on the length of ilium and vertebra. The tail is short, and the caudal number is ~8. This specimen has the least number of the dorsal and presacral vertebrae in all dicynodonts with known numbers (Liu, 2021).

The sternum is only observed in IVPP V 6033 (Fig. 16A, B). It is well ossified, but only a small portion is preserved. It is tentatively identified as the anterior-left portion. There is a mid-keel on the ventral surface while there is a wide ridge on the dorsal surface.

Pectoral girdles The scapulae are preserved in IVPP V 6033, V 11676, and V 30726 (Fig. 16). It is a narrow, gently arched bone with a dorsally expanding blade. On the anterior margin, below the upper edge of the blade, a sharp ridge runs downwards to the acromion and goes from more laterally directed to more anteriorly directed. The ventral margin of the acromion is directed slightly ventrally. A depression lies between the ridge and the blade. In

the right scapula of V 11676, the scapular ventral margin is smoothly convex, and the lateral surface is smooth too. However, this could not be deformed based on the left scapula. The ventral portion below the acromion should be much thinner than the glenoid as in V 6033 (Fig. 16E, F). A groove separates the anterior portion from the posterior portion (with glenoid) on the medial side, and a shallow notch presents on the ventral side of the groove, similar to *Wadiasaurus* (Bandyopadhyay, 1988) and less developed than *Turfanodon* (Liu, 2021).

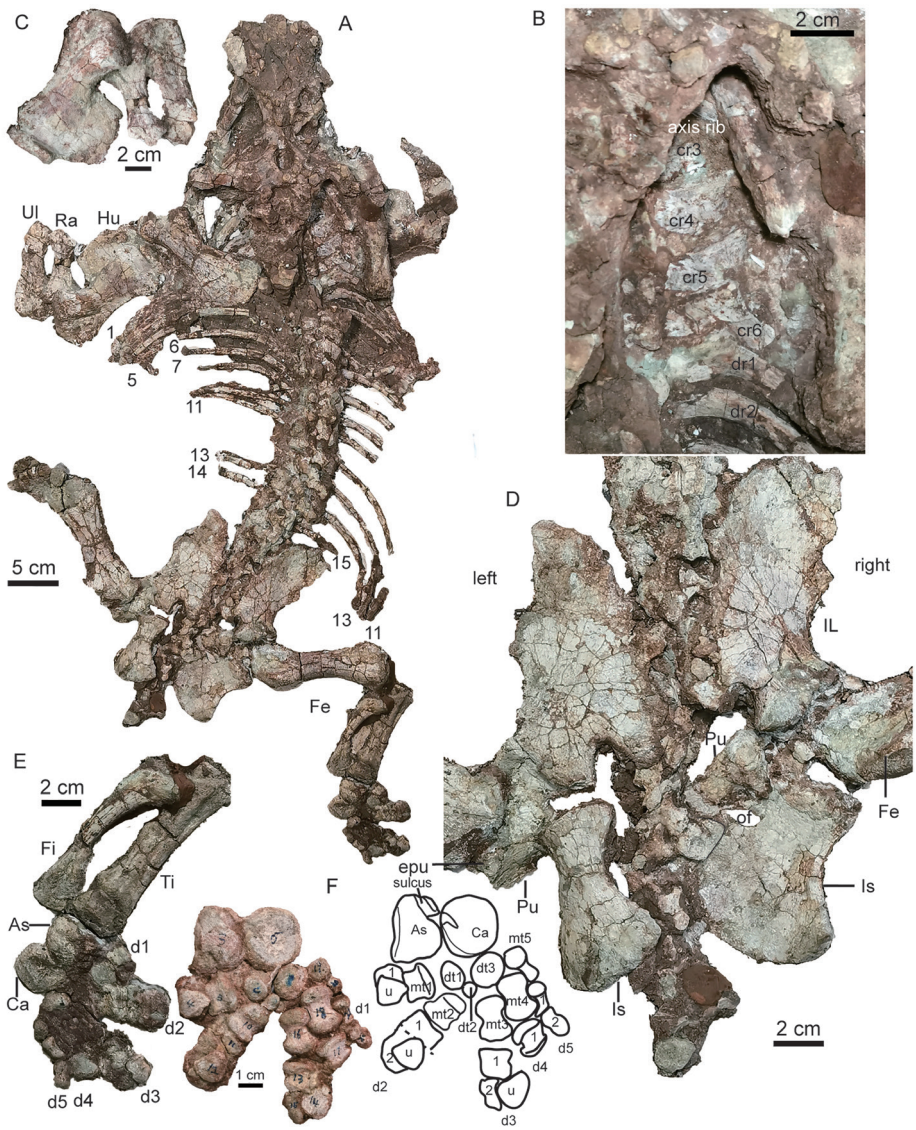

Fig. 15 *Shaanbeikannemeyeria xilougouensis* from the Ermaying Formation (IVPP V 30726)
A. skeleton in dorsal view; B. right anterior presacral ribs, C. left forelimb, humerus in lateral and slightly dorsal view, ulna and radius in lateral view; D. left pelvic girdle in lateral view, right ilia in lateral view, right pubis and ischium in medial view; E. right hind limb, tibia and fibula in anterior view, pes in dorsal view; F. photo and drawing of right pes mainly in ventral view
The numbers in (A) mark the dorsal ribs

Fig. 16 *Shaanbeikannemeyeria xilougouensis* from the Ermaying Formation, postcranial bones
IVPP V 6033: incomplete sternum in ventral (A) and dorsal (B) views; right clavicle in anterior (C) and posterior (D) views; right scapula in medial (E) and lateral (F) views
IVPP V 11676: right scapula in medial (G) and lateral (H) views; right clavicle and interclavicle in ventral (I) and dorsal (J) views; left humerus in ventral (K), dorsal (L), anterior (M) and posterior (N) views
IVPP V 30726: left scapula in lateral (O) view. Scale bars equal 2 cm

Both clavicles are preserved in V 6033 and V 11676 (Fig. 16), but only the right clavicle of V 6033 is nearly complete and is described here. The dorsal portion is slighter wider than the ventral portion. The dorsal end is wide, while the medial end has a triangular shape, quite different from those in *Sinokannemeyeria*, which has a sharp dorsal process and a narrow medial end (Sun, 1963). The articular groove with the interclavicle is indistinct. The dorsal portion is incomplete, and the medial (ventral) end is more obtuse in V 11676.

The incomplete interclavicle is attached to the dorsal surface of the right clavicle in V 11676 (Fig. 16I, J). A boss is developed along the midline, and the dorsal surface is smoothly concave.

Forelimb The humerus, ulna, and radius are preserved in IVPP V 6033 and V 30726, while only humeri are preserved in V 11676 (Figs. 15–17).

The humerus is nearly flat, even accounting for the incomplete deltopectoral crest in IVPP V 6033 (Fig. 17). However, this should be artifact because the distal end is twisted related to the proximal end in small specimens. The articular surface on the proximal head is convex and slightly expanded dorsally. The proximal end for the insertion of M. subcoracoscapularis is poorly preserved, but it is a rounded and rugose area. Distally, there is a dorsoventrally flattened area for the insertion of M. latissimus dorsi. More distally, the

Fig. 17 *Shaanbeikannemeyeria xilougouensis* from the Ermaying Formation (IVPP V 6033), limbs
Right humerus in ventral (A) and dorsal (B) views; left radius in proximal (C), anterior (D) and posterior (E) views; right ulna in medial (F) and lateral (G) views; left ulna in lateral (H) and medial (I) views; Left femur in ventral (J) and dorsal (K) views; fibula in medial (L) and lateral (M) views; left tibia in anterior (N), medial (O), posterior (P) and lateral (Q) views. Scale bars equal 2 cm

entepicondylar foramen lies at the mid-shaft. The deltopectoral crest has a thick and rough (ventral) edge which forms an obtuse angle with the distal edge. The ectepicondyle is wider than the entepicondyle. The supinator process is undeveloped in IVPP V 11676 and V 30726 but present in V 6033 (Figs. 15, 16). The articular surface on the distal end has little exposure on the dorsal surface.

The ulna is a robust bone with an anteroposteriorly compressed shaft (Fig. 17). There is no evidence for the presence of the olecranon process as a separate ossification. The olecranon process is low and rounded, similar to *Kannemeyeria simocephalus* (Govender, 2005), but quite different from that of *Sinokannemeyeria* and *Wadiasaurus* (Sun, 1963; Bandyopadhyay, 1988). The sigmoid notch is a gently concave and has a slightly elongated surface. Below the sigmoid notch, there is a facet for reception of the lateral extension of the radius. It is only observed on the right ulnae of V 6033, and it is covered by the radius on the left side of V 30726.

The radius is shorter than the ulna (Fig. 17). It has a slender shaft and expanded ends. The proximal end is a shallow concave surface surrounded by a prominent rim. Below the proximal end, a rugose surface presents on the posterolateral side, part of it for the facet on the proximal end of the ulna. The anterior surface is flat and the posterior surface is convex and bears a ridge which runs proximodistally. The distal end is an oval concave surface for the articulation of the radiale.

The pelvic girdle All pelvic bones are preserved in IVPP V 30726 (Fig. 15D). The ilia are exposed in lateral view and the left pubis and ischium are mainly exposed in lateral view, while the right pubis and ischium are in medial view.

The ilium has a flat, thin, dorsomedially orientated plate, iliac blade. The iliac anterior process is much longer than the posterior process, which is short and tapers almost to a point. The blade constricts to the neck which is as wide as the acetabulum. Ventrally, the bone thickens and expands, bearing the acetabular facet laterally and the facets for the pubis anteroventrally and ischium posteroventrally. The medial surface is not exposed, but it should bear facets for at least five sacral ribs.

The pubis is a thick but short bone. It is fused to the ischium as one plate on the right side, but is separated on the left side. It has a concave lateral surface. The anterior edge is poorly known, but its unfinished rough end, the area for the cartilaginous epipubis, is exposed. The posterior margin is notched in the middle for the obturator foramen.

The ischium is broad with a convex outer surface and concave inner surface. Below the acetabular part, the anterior margin is deeply notched for the obturator foramen, below which this margin meets the pubis. The bone is thickened posteriorly and forms a posterodorsal flange.

Hind limb The right hind limb is nearly complete in IVPP V 30726 (Fig. 15), while femur, tibia, and fibula are preserved in V 6033 (Fig. 17).

Both femora of V 30726 are articulated to the acetabulum and almost exposed in dorsal view (Fig. 15). The left femur of V 6033 is nearly complete, with a length of 25 cm (Fig. 17J, K). The proximal expansion is as wide as the distal. The head is a moderate swelling on the dorsal margin, although not so rounded, but it slightly encroaches on the anterior surface. The trochanter major has a rugose surface and is slightly convex outwards. This area has many striae but is smoother in the young specimen (V 30726). The insertion of M. iliofemoralis is a distinct crest on the lateral surface. The intertrochanteric fossa is shallow. The shaft is flattened with a smallest width of 5 cm. Distally, the articulating condyles are well developed, while the posterior condyle is larger and more rounded. The ventral articulating surfaces of the condyles are nearly at the same level. The popliteal fossa is shallow and wide.

The fibula is slender and bows laterally somewhat away from tibia (Fig. 15E). It also bows anteriorly. The ends are slightly expanded.

The tibia is a robust bone and expanded proximally to form articular facets for two femoral condyles, which are concave and separated by a prominent crest (Figs. 15E, 17N–Q). The proximal side of the bone is expanded anterolaterally as the cnemial crest, which narrows ventrally and disappears before it reaches half the length. A wide groove lies between the cnemial crest and the lateral margin. The shaft becomes narrow in the middle. The medial/posterior margin of the bone is strongly concave, while the lateral/anterior margin is nearly straight. The distal end is less expanded than the proximal, and the distal articular facet is oval, slightly concave in the lateral half, and convex in the medial.

The right pes was rotated relative to the tibia and fibula (Fig. 15E). Most elements are preserved and mainly exposed in ventral view while digital V is exposed in lateral view, only 3 phalanges of digital IV and V are lost (Fig. 15F).

The astragalus and calcaneum are articulated to each other, the former partially covers the latter in dorsal view (Fig. 15E). Two bones are similar in size, but the astragalus is near square and much thicker. The proximal articular facet for the tibia is convex. A distinct sulcus runs from proximal corner to the lateral margin on the ventral surface towards the calcaneum. The calcaneum is a rounded plate that is thin in the middle but with thickened margins, especially the medial margin. A shallow depression presents on the middle in both the dorsal and ventral surfaces. A shallow notch is present on the medial margin of the ventral surface, connecting to the astragalus sulcus. Three distal tarsal are ossified and are ellipsoid in shape. The distal tarsal 3 is the largest in size while the distal tarsal 2 is the smallest. The distal tarsal 3 articulates to metatarsals 3, 4 and 5.

The metatarsals are broad, short, and constrict in the middle. The articulating surfaces on the two sides are transversely elongated. They vary in length: metatarsals 3, 4 are longest, while metatarsal 1 is the shortest but broadest.

The preserved digital formula is 2-3-3-1-2, fitting to the general dicynodont digital formula. Except for the ungual ones, the phalanges are quite broad and short. They are

shorter than the respective metatarsals. The last ungual phalanx turns back and ventral to the penultimate phalange in digital I to III. The ungual phalanges are spatulate and end in rounded tips.

Kannemeyeriiformes

?*Parakannemeyeria* Sun, 1960

Referred specimen IVPP V 30727 and V 30730, two partial postcranial skeletons.

Comments The postcranial bones of V 30730 are slightly larger than the corresponding bones in V 30726 and V 11676. Although it is associated with a juvenile skull (V 30729), the skull size is too small when compared with V 11676 and V 30726, so they should belong to different individuals.

Description IVPP V 30730 comprises of 10 vertebrae, some ribs, the left ilium, femur, tibia, and fibula (Fig. 18A–D). V 30727 includes some dorsal vertebrae and ribs, paired pectoral girdles, humeri, the right ulna and right radius (Fig. 18E–N).

In IVPP V 30727, 8 dorsal centra are exposed and more than 6 ribs are preserved. In V 30730, the last 6 dorsal and first 4 sacral vertebrae are preserved (Fig. 18B, D). The dorsal centra are roughly 2 cm in length in both specimens. This indicates that they are similar in size. In V 30730, the short ribs are fused to the neural arches. The vertebrae are compressed, so the ribs nearly lie on a plane with the poorly preserved neural spines. Three right sacral ribs are present. The distal end of the first one is extremely expanded and its width (28 mm) is much greater than the length of the sacral vertebra (21 mm).

The preserved pectoral girdle elements include right scapula, coracoid, and procoracoid (Fig. 18E, F). The scapula measures 17 cm in height, taller than that of V 11675. The posterior side is incomplete, but the preserved portion is similar to that of V 6033 (Fig. 16). The coracoid plate is composed of coracoid and procoracoid, which are sutured together. The glenoid is manly formed by the scapula and the coracoid, but the posterodorsal margin of the procoracoid also contributes a small portion. The coracoid foramen lies entirely within the procoracoid and close to the posterodorsal corner of the bone. On its medial surface, the coracoid foramen opens dorsally as a groove and continuous to the scapular groove. The procoracoid is broken for most of its free margin, while the ventral margin of the coracoid plate is smoothly convex. The coracoid has a long posteroventral process, more similar to *Parakannemeyeria youngi* (IVPP V 972) than *Sinokannemeyeria* (Young, 1937; Sun, 1963).

The right humerus is relatively complete except for the deltopectoral crest (Fig. 18G, H). This bone is longer than that of IVPP V 11676 and V 30726, but it is thinner and more slender, and the shaft also is narrower (24 mm in narrowest place in dorsal view) than described above. The two extremities are poorly ossified, indicating a young stage of the bone. The deltopectoral crest forms a big angle with the head, indicating no distinct deformation. A bone is identified as the right radius here (Fig. 18I–K). It has a concave area close to the proximal

end, which should not be present here, and it is explained as the result of the poor ossification of the extremities and deformation during the preservation. The right ulna has a poorly ossified proximal end and has lost the distal end (Fig. 18L, M). The articular facet for the humerus is poorly developed.

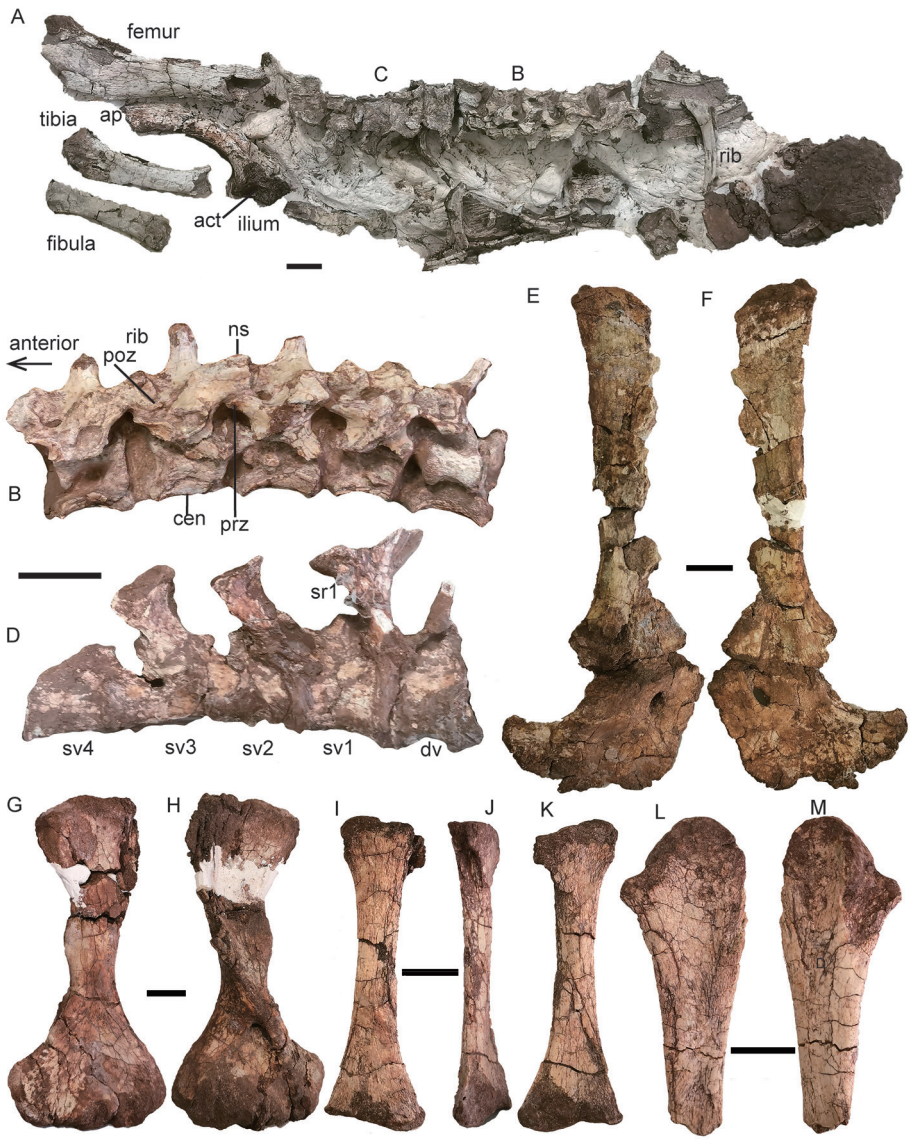

Fig. 18 ?*Parakannemeyeria* from the lower portion of the Ermaying Formation
IVPP V 30730: A. partial posterior skeleton in dorsal view; B. five dorsal vertebrae and associated ribs in left dorsolateral view; C, D. last dorsal vertebra and four sacral vertebrae and associated ribs in left dorsolateral (C) and ventral (D) views
IVPP V 30727: E, F. right scapula, procoracoid and metacoracoid in lateral (E) and medial (F) views; G, H. right humerus in dorsal (G) and ventral (H) views; I–K. right radius in anterior (I), medial (J), and posterior (K) views; L, M. right ulna in posterior (L) and anterior (M) views. Scale bars equal 2 cm

The left ilium preserves the anterior process of the blade and the ventral portion for the articulation of ischium, pubis and femur (Fig. 18A). The iliac facet of the acetabulum faces ventrally for the most part, its lateral rim projects laterally, and the anterior and posterior rims form a sharp angle. The femur, tibia, and fibula are incomplete, both losing the proximal and distal ends. They are longer but more slender than the corresponding bones of IVPP V 30726.

Discussion Four kannemeyeriid genera are known in China: *Sinokannemeyeria*, *Parakannemeyeria*, and *Shaanbeikannemeyeria* from North China, and *Xiyukannemeyeria* from Xinjiang (Li and Liu, 2015). The coracoid shows the difference from *Sinokannemeyeria*. The humerus is more slender than the similar size humerus of *Xiyukannemeyeria* (Sun, 1978). All limb bones are longer but more slender than the corresponding bones in IVPP V 11676 and V 30726. These bones are poorly ossified at their extremities, indicating a young age. All known features of these specimens are consistent with *Parakannemeyeria youngi* (Sun, 1963), and this genus was also reported from the lower Ermaying Formation (Cheng, 1980), so they are tentatively referred to *Parakannemeyeria*.

6 Phylogenetic analysis of *Shaanbeikannemeyeria*

To test the phylogenetic position of *Shaanbeikannemeyeria*, it was recoded based on the available specimens for the revised character list based on Angielczyk et al. (2021), Kammerer and Ordoñez (2021), and Liu (2021) (Supplementary file 2). *Turfanodon jiufengensis* and *Kunpania scopulusa* are also coded and added to the matrix. The final data set consists of 119 operational taxonomic units (OTUs) and 199 characters (23 continuous and 176 discrete-states) (Supplementary file 3). Continuous characters were treated as additive, and eight discrete-state characters were treated as ordered (characters 56, 81, 84, 102, 163, 173, 189 and 199). The data were analyzed using parsimony in TNT v1.5 (Goloboff and Catalano, 2016), resulting in one most parsimonious tree of length 1267.069.

The tree is mostly identical to that of Kammerer and Ordonez (2021) except for the interrelationships within clade A (Kannemeyeriidae), L (*Lystrosaurus*), and P (Placeriinae) (Fig. 19). In recent analyses, Kannemeyeriiformes includes non-monophyletic shansiodontids plus two major clades: the Kannemeyeriidae and another clade (B) including the Stahleckeriidae as subclade (Angielczyk et al., 2017; Kammerer et al., 2019; Kammerer and Ordoñez, 2021; Liu, 2021) (Fig. 19). Although the members of Kannemeyeriidae are stable, the interrelationships of different taxa vary a lot. For example, *Kannemeyeria* as a monophyletic genus was recovered by Kammerer & Ordoñez (2021); *Shaanbeikannemeyeria* is an early divergent taxon (Angielczyk et al., 2017; Kammerer et al., 2019), or forms the sister taxon of *Rechnisaurus* plus *Uralokannemeyeria*.

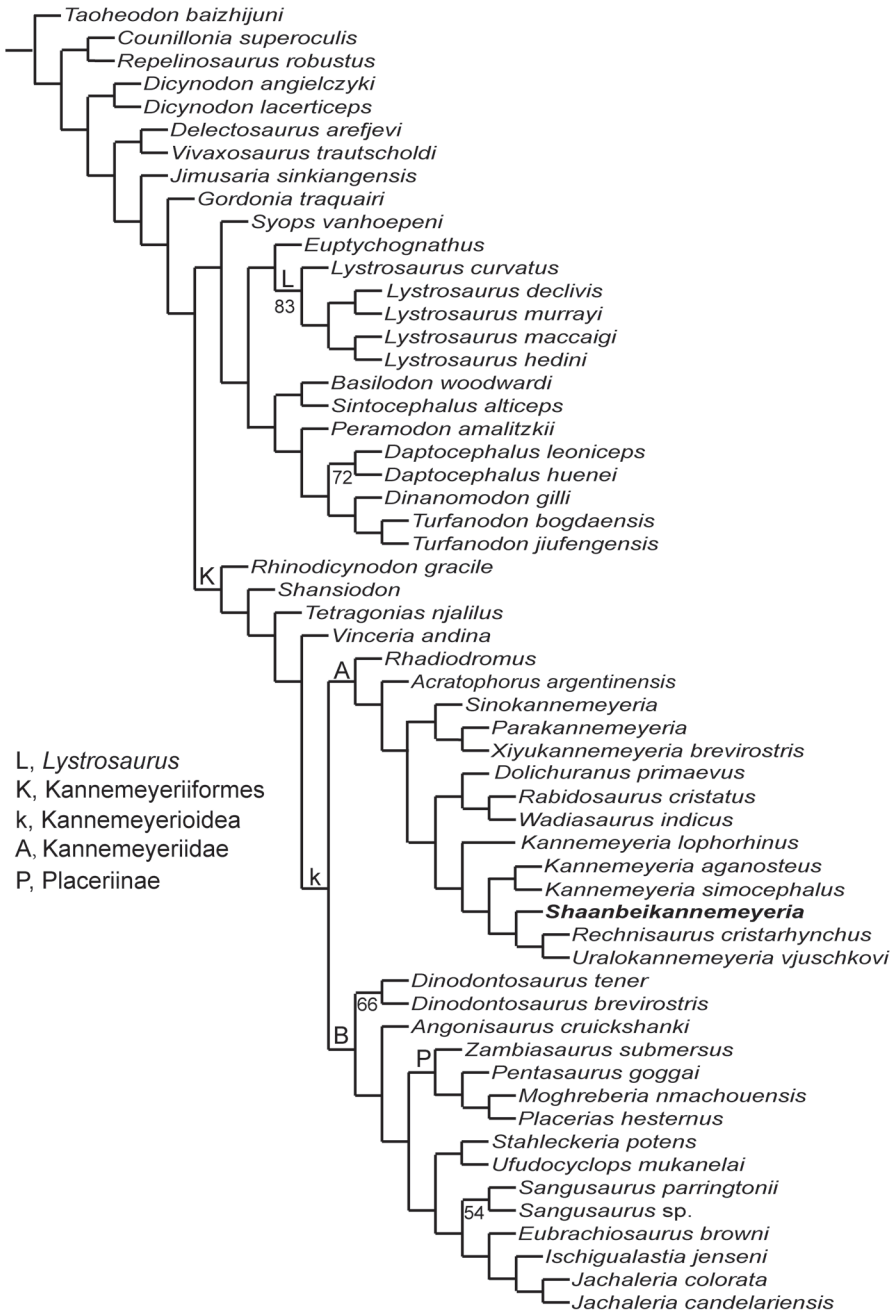

Fig. 19 Results of the phylogenetic analysis, showing the interrelationships within Dicynodontoidea
Numbers below nodes represent symmetric resampling values

7 Discussion

7.1 Diagnostic features of *Shaanbeikannemeyeria xilougouensis*

The premaxillary posterodorsal processes are sword tip-like in *Shaanbeikannemeyeria*,

different from the nearly triangular ones in most Triassic kannemeyeriiforms, such as *Vinceria* (Bonaparte, 1969; Domnanovich and Marsicano, 2012), *Shansiodon* (Cheng, 1980), *Tetragonias* (Cruickshank, 1967), *Rhinodicynodon* (Kalandadze, 1970), *Acratophorus* (Kammerer and Ordoñez, 2021), *Sinokannemeyeria* (Sun, 1963), *Parakannemeyeria* (Sun, 1960; Sun, 1963); *Xiyukannemeyeria* (Liu and Li, 2003), *Rhadiodromus* (Surkov, 2003), *Rechnisaurus* (Bandyopadhyay, 1989), *Wadiasaurus* (Bandyopadhyay, 1988), *Kannemeyeria* (Renaut and Hancox, 2001), *Dolichuranus* (Damiani et al., 2007), *Rabidosaurus* (Kalandadze, 1970), *Ufudocyclops* (Kammerer et al., 2019), *Dinodontosaurus* (von Huene, 1935; Cox, 1968; Morato, 2006), *Stahleckeria* (Maisch, 2001; Vega-Dias et al., 2005); from quite narrow in *Ischigualastia* (Kammerer and Ordoñez, 2021). This process is absent in *Jachaleria* (Araújo and Gonzaga, 1980; Vega-Dias and Schultz, 2004), unsure in *Angonisaurus* (Cox and Li, 1983), *Sangusaurus* (Angielczyk et al., 2017; Kammerer and Ordoñez, 2021), *Uralokannemeyeria* (Danilov, 1971), *Moghreberia* (Dutuit, 1988), and unknown in *Eubrachiosaurus* (Williston, 1904; Kammerer et al., 2013), *Zambiasaurus* (Cox, 1969), and *Pentasaurus* (Kammerer, 2018).

The dentary of *Shaanbeikannemeyeria* has a tall, dorsally-convex cutting blade on the medial edge of the dorsal surface (Character 149). This state is only present in some Permian dicynodonts such as *Diictodon* (Sullivan and Reisz, 2005), *Robertia* (King, 1981), but unreported in Triassic dicynodonts.

The reflected lamina of the angular of *Shaanbeikannemeyeria* is generally similar to that of *Acratophorus argentinensis* or *Kannemeyeria simocephalus*: large, rounded, and the ventral portion has a concave lateral surface (Renaut and Hancox, 2001; Kammerer and Ordoñez, 2021). It is different from that of *Sinokannemeyeria* or *Parakannemeyeria* in which it is elongated and the ventral portion has a convex surface (Sun, 1963). However, the ventral portion is separated as a small posteroventral directed process in this taxon.

Shaanbeikannemeyeria shares the following features with *Kannemeyeria*, *Rechnisaurus* and *Uralokannemeyeria*: the posterior pterygoid rami form a big angle (>98º) (C9), the palatal surface of premaxilla is exposed in lateral view (C44), and a median snout ridge is present on the premaxilla and nasal (C199). The angle formed by the two posterior pterygoid rami (~115º) is largest in *Shaanbeikannemeyeria* (Supplementary file 4).

Shaanbeikannemeyeria shares the following features with *Rechnisaurus* and *Uralokannemeyeria*: the preorbital region is nearly more than half the basal length of the skull (C1), the occiput is inclined relative to palate so to have a short skull basal length (C13), the snout anterior tip is squared off (C35), the parietals are exposed in midline groove or channel (C72), the caniniform process lies slightly below the anterior extended line of the zygomatic arch and the dorsal edge of the erupted portion of the canine tusk anterior to the anterior naris margin (C55), with wide lateral extension so exposed in dorsal view, and the ventral surface of the median pterygoid plate has a thin median ridge (C115, unknown in *Rechnisaurus*). However, the occiput is strongly inclined in *Shaanbeikannemeyeria*, so it has the shortest basal

length compared to dorsal length in all known kannemeyeriiforms. *Shaanbeikannemeyeria* also has the longest preorbital region related to the skull basal length, but it is possibly related to its short skull basal length. It differs from *Uralokannemeyeria* and *Rechnisaurus* by the postorbital not extending the entire length of intertemporal bar and oblique ridge on lateral side of zygomatic arch in adult.

Shaanbeikannemeyeria is easy to distinguish from other Triassic kannemeyeriiform from North China (*Shansiodon*, *Sinokannemeyeria*, *Parakannemeyeria*) based on the complete cranial material by the strongly inclined occiput. For incomplete specimens, it also can be differentiated from them by the sword tip-like premaxillary posterodorsal processes, the dorsally-convex cutting blade on medial edge of dorsal surface of dentary, and reflected lamina with a separated posteroventral process. It is differentiated from *Shansiodon* by its larger size, relatively small temporal fenestrae, and intertemporal bar that is wide, not crest-like, and raised from the skull roof. It is differentiated from *Sinokannemeyeria* and *Parakannemeyeria* by its short snout, premaxillary lateral surface anterior to external naris without lateral extension, small caniniform process and tusk, narrower interorbital region, and longer intertemporal bar.

7. 2 Variations within *Shaanbeikannemeyeria*

In specimens of *Shaanbeikannemeyeria*, the caniniform processes are well developed on all skulls with a basal length no less than 24 cm, while they are poorly developed in all smaller skulls. The specimens are classified into three groups based on the skull basal length (Table 1): adults (≥ 24 cm), subadults (10 cm<skull basal length < 24 cm), and juvenile (<10 cm).

A distinct feature presents in IGCAGS V315, IVPP V 6033, and V 11674: the interpterygoid vacuity lies dorsally to the anterior margin of the median pterygoid, and its anteroposterior length is much less than the width. In these specimens, the parabasisphenoid is strongly curved and nearly vertical (broken in V 11674). In IVPP V 11675, V 11677, V 17604, the parabasisphenoid is well-preserved and only slightly curved ventrally. The former could be the deformation from compression of the occiput rather than natural state. In the smaller IVPP V 11676, the parabasisphenoid is also broken possibly due to the compression. So the strongly inclined occiput in some specimens (e.g., IGCAGS V315, IVPP V 11674) could be exaggerated by the deformation, but *Shaanbeikannemeyeria* still has the strongest inclined occiput because the undeformed specimen (IVPP V 11677) still has a greatest value of character 13 (Supplementary file 4).

The specimens show many distinct variations on the cranial morphology, even among adults (Table 2). The occiput varies in the width related to the height and the holotype has the widest occiput even though its skull length is shorter than other specimens. The caniniform process is undeveloped in pre-adult specimens. The characters have a random distribution in these specimens, so it is unlikely that they represent more than one species, as in the classification of Li and Liu (2015). However, the different shape of the caniniform process can be the result of dimorphism, as showed in some Triassic dicynodont species (Kammerer and Ordoñez, 2021).

Table 2 Variations of some cranial features among different specimens

	ratio of occipital width/height	snout tip	orbital portion of the zygomatic arch	caniniform process
IGCAGS V315	1.22	obtuse	rod-like	flat
IVPP V 11674	1.20	sharp	nearly flat dorsoventrally	flat
IVPP V 6033	1.61		nearly flat dorsoventrally	rounded
IVPP V 11675			rod-like	rounded
IVPP V 11676	1.27	obtuse	rod-like	undeveloped
IVPP V 11677	1.54	sharp	rod-like	rounded

The specimens of *S. xilougouensis* also display some ontogenetic variations. The caniniform process and tusk are undeveloped in the pre-adult specimens (IVPP V 11676, V 17904, V 30726), and the dorsal edge of the erupted portion of the canine tusk still lies below the naris, but anterior to the anterior naris margin in adults. The maxillary posterior process extends only to the middle of the orbit in the small specimens (IVPP V 30725, V 30726), but extends approach or even posterior to the anterior margin of the postorbital bone in large specimens (IVPP V 11674, V 11677). The frontals are close to the premaxilla in pre-adults (IVPP V 30726, V 11676), but widely separated in adults. The intertemporal bar is wide and the parietals are well exposed in V 11676, but it turns into a narrow bar with parietals exposed in the midline groove in adults. The ectopterygoid is a distinct bone in smaller specimens but cannot be identified in the holotype. The oblique ridge is absent on the lateral side of zygomatic arch in subadults (V 11676) but present in adults. The ratio of the deltopectoral crest relative to total length of the humerus increases through ontogeny (C18, Fig. 19), while the relative orbital size, relative size of temporal fenestra, width of median pterygoid plate relative to basal skull length, and the maximum height of postdentary bones (excluding reflected lamina of angular) relative to the height of the dentary ramus decease (C16) (Supplementary file 4).

7. 3 Coexistence of two kannemeyeriiform taxa in lower Ermaying Formation

The studied cranial materials all belong to *Shaanbeikannemeyeria*. The skull of IVPP V 30726 is poorly preserved, but the available features such as the inclined occiput, pterygoid posterior rami forming a large angle are consistent with known features of *Shaanbeikannemeyeria*, and the postcranial elements are nearly identical with those of V 11676, and similar to those of V 6033. IVPP V 30727 and V 30730 represent a different taxon, possibly *Parakannemeyeria*. It should also be noted that two genera possibly also coexisted in the *Sinokannemeyeria-Shansisuchus* Assemblage Zone (Liu, 2015).

8 Conclusions

Although there are some variations in cranial and postcranial features, *Shaanbeikannemeyeria* includes only one valid species, *S. xilougouensis*. It is characterized by an occiput that is strongly inclined relative to the palate so to have a short skull basal length, sword tip-like premaxillary posterodorsal processes, a tall and dorsally-convex cutting blade on medial edge of the dorsal surface of the dentary, reflected lamina with a separated

posteroventral process, and 15 dorsal vertebrae. *S. xilougouensis* is not a basal member within the Kannemeyeriidae. Another kannemeyeriiform genus, possible *Parakannemeyeria*, coexisted with *Shaanbeikannemeyeria* in the lower Ermaying Formation.

Acknowledgments Thanks to all colleagues contributed to the collecting of the specimens (LI Jin-Ling, Wu Xiao-Chun, Tang Zhi-Lu, Gao Ke-Qin, Hou Lian-Hai, Zhu Yang-Long, Feng Wen-Qing, Li Qiang, Liu Yi-Hong, Lou Yu-Shan). Some specimens were prepared by Xu Xu, Wu Yong, Liu Yu-Dong, and Lan Li-Li. The geological column is drawn by Yi Jian. Thanks to Kenneth Angielczyk for the discussion on character coding, Yinmai O'Connor for checking the grammar. The comments from K. Angielczyk and Christian Kammerer significantly improved this paper. This work was supported by the Strategic Priority Research Program of the Chinese Academy of Sciences (XDB26000000), the International Partnership Program of the Chinese Academy of Sciences, (No. 132311KYSB20190010).

Supplementary material can be found on the website of Vertebrate PalAsiatica (http://www.vertpala.ac.cn/EN/2096-9899/home.shtml) in advanced online publication.

鄂尔多斯盆地陕北肯氏兽组合带的肯氏兽型二齿兽类

刘 俊[1,2]

(1 中国科学院古脊椎动物与古人类研究所，中国科学院脊椎动物演化与人类起源重点实验室 北京 100044)

(2 中国科学院大学地球与行星科学学院 北京 100049)

摘要：陕北肯氏兽是二马营组下部常见的四足动物。这个属在分类学上还有一些问题没有解决，例如本属是否有效，包括几个种等。自1978年以来又陆续采集到一些材料。陕北肯氏兽首现于和尚沟组顶部。描述了发现的所有陕北肯氏兽化石，厘清其鉴定特征，了解个体差异，确认其系统位置。陕北肯氏兽只包含一个有效种：戏楼沟种，其独有衍征包括：枕部相对腭部强烈倾斜因而头骨腹面短，前颌骨有剑尖状的后背突，齿骨背侧内缘呈背凸的刀片状，隅骨的反折翼有一独立的后腹突，15枚背椎。这一属种在头骨形态上存在个体间差异，例如枕高相对枕宽比、吻尖形态(尖或钝)、颧弓眼眶部分形状以及齿突形态。有些差异可能与个体发育有关，例如齿突和长牙的发育程度、前颌骨在颧弓上向后延伸程度、前颌骨与额骨的距离、间颞部宽度及顶骨出露程度。基于头后骨骼可以判定二马营组下部还存在第二种肯氏兽类，可能是副肯氏兽。

关键词：和尚沟组，二马营组，中三叠世，安尼期，肯氏兽型类

References

Angielczyk K D, Hancox P J, Nabavizadeh A, 2017. A redescription of the Triassic kannemeyeriiform dicynodont *Sangusaurus* (Therapsida, Anomodontia), with an analysis of its feeding system. J Vert Paleont, 37(sup1): 189–227

Angielczyk K D, Liu J, Yang W, 2021. A redescription of *Kunpania scopulusa*, a bidentalian dicynodont (Therapsida, Anomodontia) from the ?Guadalupian of northwestern China. J Vert Paleont, 41(1): e1922428

Araújo D C, Gonzaga T D, 1980. Uma Nova especie de Jachaleria (Therapsida, Dicynodontia) do Triassico do Brasil. Actas del Segundo Congreso Argentino de Paleontologia y Bioestratigrafia y Primer Congreso Latino Americano de Paleontologia, 2, tome 1, Buenos Aires. 159–174

Bandyopadhyay S, 1988. A kannemeyeriid dicynodont from the Middle Triassic Yerrapalli Formation. Philos Trans R Soc Lond B Biol Sci, 320: 185–233

Bandyopadhyay S, 1989. The mammal–like reptile *Rechnisaurus* from the Triassic of India. Palaeontology, 32: 305–312

Bonaparte J F, 1969. Dos nuevas “faunas” de reptiles triásicos de Argentina. In: Amos A J ed. Gondwana Stratigraphy, IUGS Symposium, Buenos Aires, 1–15. Paris: UnitedNations Educational Scientific and Cultural Organization, 283–306

Cheng Z W, 1980. 7. Vertebrate fossils. In: Mesozoic Stratigraphy and Palaeontology of the Shaanxi–Gansu–Ninxia Basin. Beijing: Geological Publishing House. 115–188

Cox C B, 1959. On the anatomy of a new dicynodont genus with evidence of the position of the tympanum. Proc Zool Soc London, 132(3): 321–367

Cox C B, 1968. The Chañares (Argentina) Triassic reptile fauna; IV, The dicynodont fauna. Breviora, 295: 1–27

Cox C B, 1969. Two new dicynodonts from the Triassic Ntawere Formation, Zambia. Bull Br Mus Nat Hist Geol, 17: 257–294

Cox C B, 1991. The Pangaea Dicynodont *Rechnisaurus* and the Comparative Biostratigraphy of Triassic Dicynodont Faunas. Palaeontology, 34: 767–784

Cox C B, Li J L, 1983. A new genus of Triassic dicynodont from East Africa and its classification. Palaeontology, 26: 389–406

Cruickshank A R I, 1967. A new *Dicynodont* genus from the Manda Formation of Tanzania (Tanganyika). J Zool, 153: 163–208

Damiani R J, Vasconcelos C, Renaut A et al., 2007. *Dolichuranus primaevus* (Therapsida : Anomodontia) from the Middle Triassic of Namibia and its phylogenetic relationships. Palaeontology, 50: 1531–1546

Danilov A I, 1971. A new dicynodont from the Middle Triassic of southern Cisuralia. Paleontol J, 5(2): 265–268

Domnanovich N S, Marsicano C A, 2012. The Triassic dicynodont Vinceria (Therapsida, Anomodontia) from Argentina and a discussion on basal Kannemeyeriiformes. Geobios, 45(2): 173–186

Dutuit J M, 1988. Ostéologie crânienne et ses enseignements, apports géologique et paléoécologique, de *Moghreberia nmachouensis*, Dicynodonte (Reptilia, Therapsida) du Trias supérieur marocain. Bull Mus Nat Hist Nat, 10: 227–285

Goloboff P A, Catalano S, 2016. TNT, version 1.5, with a full implementation of phylogenetic morphometrics. Cladistics, 32: 221–238

Govender R, 2005. Morphological and functional analysis of the postcranial anatomy of two dicynodont morphotypes from the *Cynognathus* assemblage zone of South Africa and their taxonomic implications. Ph. D thesis. University of the Witwatersrand. 1–199

Kalandadze N N, 1970. New Triassic kannemeyeriids from South Cisuralia. In: Flerov K K ed. Materials on the Evolution of Terrestrial Vertebrates. Moscow: Nauka. 51–57

Kammerer C F, 2018. The first skeletal evidence of a dicynodont from the lower Elliot Formation of South Africa. Palaeontol Afr, 52: 102–128

Kammerer C F, Ordoñez M d l A, 2021. Dicynodonts (Therapsida: Anomodontia) of South America. J South Am Earth Sci, 108: 103171

Kammerer C F, Fröbisch J, Angielczyk K D, 2013. On the validity and phylogenetic position of *Eubrachiosaurus browni*, a kannemeyeriiform dicynodont (Anomodontia) from Triassic North America. PLoS ONE, 8(5): e64203

Kammerer C F, Viglietti P A, Hancox P J et al., 2019. A new kannemeyeriiform dicynodont (*Ufudocyclops mukanelai*, gen. et sp. nov.) from Subzone C of the *Cynognathus* Assemblage Zone, Triassic of South Africa, with implications for biostratigraphic correlation with other African Triassic Faunas. J Vert Paleont, 39(2): e1596921

King G M, 1981. The postcranial skeleton of *Robertia broomiana*, an early dicynodont (Reptilia, Therapsida) from the South African Karoo. Ann S Afr Mus, 84(5): 203–231

King G M, 1988. Anomodontia. Stuttgart: Gustav Fischer Verlag. 1–174

Li J L, 1980. *Kannemeyeria* Fossil from Inner Mongolia. Vert PalAsiat, 18(2): 94–99

Li J L, Cheng Z W, 1995. A new Late Permian vertebrate fauna from Dashankou, Gansu, with comments on Permian and Triassic vertebrate assemblage zones of China. In: Sun A L, Wang Y Q eds. Sixth Symposium on Mesozoic Terrestrial Ecosystems and Biota, Short Papers. Beijing: China Ocean Press. 33–37

Li J L, Liu J, 2015. Basal Synapsids. Palaeovertebrate Sinica, III(14): 105

Liu J, 2015. New discoveries from the *Sinokannemeyeria-Shansisuchus* Assemblage Zone: 1. Kannemeyeriiformes from Shanxi, China. Vert PalAsiat, 53(1): 16–28

Liu J, 2018. New progress on the correlation of Chinese terrestrial Permo–Triassic strata. Vert PalAsiat, 56(4): 327–342

Liu J, 2021. The tetrapod fauna of the upper Permian Naobaogou Formation of China: 6. *Turfanodon jiufengensis* sp. nov. (Dicynodontia). PeerJ, 9: e10854

Liu J, Li J L, 2003. A new material of kannemeyerid from Xinjiang and the restudy of *Parakannemeyeria brevirostris*. Vert PalAsiat, 41(2): 147–156

Liu J, Ramezani J, Li L et al., 2018. High–precision temporal calibration of Middle Triassic vertebrate biostratigraphy: U–Pb zircon constraints for the *Sinokannemeyeria* Fauna and *Yonghesuchus*. Vert Palasiat, 56(1): 16–24

Lucas S G, 2001. Chinese Fossil Vertebrates. New York: Columbia University Press. 1–375

Maisch M W, 2001. Observations on Karoo and Gondwana vertebrates. Part 2: A new skull–reconstruction of Stahleckeria potens von Huene, 1935 (Dicynodontia, Middle Triassic) and a reconsideration of kannemeyeriiform phylogeny. Neues Jahrb Geol P–A, 220(1): 127–152

Morato L, 2006. *Dinodontosaurus* (Synapsida, Dicynodontia) reconstituições morfológicas e aspectos biomecânicos. Master thesis. Porto Alegre (RS): Universidade Federal do Rio Grande do Sul. 1–158

Olson E C, 1944. Origin of mammals based upon cranial morphology of the therapsid suborders. Geol Soc Am Spec Pap, 55: 1–136

Owen R, 1860. On the orders of fossil and recent Reptilia, and their distribution in time. Report of the Twenty–Ninth Meeting of the British Association for the Advancement of Science, 1859: 153–166

Renaut A J, Hancox P J, 2001. Cranial description and taxonomic re–evaluation of *Kannemeyeria argentinensis* (Therapsida: Dicynodontia). Palaeontol Afr, 37: 81–91

Sullivan C, Reisz R R, 2005. Cranial anatomy and taxonomy of the Late Permian dicynodont Diictodon. Ann Carnegie Mus, 74(1): 45–75

Sun A L, 1960. On a new genus of kannemeyerids from Ningwu, Shanxi. Vert PalAsiat, 4(2): 67–80

Sun A L, 1963. The Chinese kannemeyerids. Palaeont Sin, New Ser C, 17: 1–109

Sun, A L, 1978. Discovery of *Parakannemeyeria* from Xinjiang. Mem Inst Vert Paleont Paleoanthrop, Acad Sin, 13, 47–54

Surkov M V, 2003. A new anomodont (Therapsida) from the Middle Triassic of the southern Fore–Urals. Paleontol J, 37(4): 425–431

Vega–Dias C, Schultz C L, 2004. Postcranial material of *Jachaleria candelariensis* Araújo and Gonzaga 1980 (Therapsida, Dicynodontia), Upper Triassic of Rio Grande do Sul, Brazil. PaleoBios, 24(1): 7–31

Vega–Dias C, Maisch M W, Schwanke C, 2005. The taxonomic status of *Stahleckeria impotens* (Therapsida, Dicynodontia): redescription and discussion of its phylogenetic position. Rev Bras Paleontol, 8(3): 221–228

von Huene F F, 1935. Die fossilen Reptilien des südamerikanischen Gondwanalandes. Ergebnisse der Sauriergrabungen in Südbrasilien, 1928-1929. Ordnung Anomodontia. Munich: C. H. Beck'sche Verlagsbuchhandlung. 1–92

Williston S W, 1904. Notice of some new reptiles from the Upper Trias of Wyoming. J Geol, 12(8): 688–697

Young C C, 1937. On the Triassic dicynodonts from Shansi. Bull Geol Soc China, 17: 393–411